TRIBHUVAN UNIVERSITY

INSTITUTE OF ENGINEERING

PULCHOWK CAMPUS

THESIS NO: 076/MSPSE/003

Battery Energy Storage System for Reducing the Impact of Renewable Energy Sources Penetration on Frequency Regulation

by

Ashutosh Kumar Jha

A THESIS

SUBMITTED TO THE DEPARTMENT OF ELECTRICAL ENGINEERING

IN PARTIAL FULFILMENT OF THE REQUIREMENTS FOR THE

DEGREE OF MASTER OF SCIENCE IN POWER SYSTEM ENGINEERING

DEPARTMENT OF ELECTRICAL ENGINEERING

LALITPUR, NEPAL

September, 2022

Battery Energy Storage System for Reducing the Impact of Renewable Energy Sources Penetration on Frequency Regulation

by

Ashutosh Kumar Jha

(076MSPSE003)

Thesis Supervisor

Associate Prof. Jeetendra Chaudhary

Assistant Prof. Akhileshwar Mishra

A thesis submitted in partial fulfilment of the requirements for the degree of Master of Science in Power System Engineering

Department of Electrical Engineering

Institute of Engineering, Pulchowk Campus

Tribhuvan University

Lalitpur, Nepal

September, 2022

COPYRIGHT

TRIBHUVAN UNIVERSITY

INSTITUTE OF ENGINEERING

PULCHOWK CAMPUS

DEPARTMENT OF ELECTRICAL ENGINEERING

The undersigned certify that they have read, and recommended to the Institute of Engineering for acceptance, a thesis entitled **" Battery Energy Storage System for Reducing the Impact of Renewable Energy Sources Penetration on Frequency Regulation"** submitted by **Ashutosh Kumar Jha** in partial fulfillment of the requirements for the degree of Master of Science in Power System Engineering.

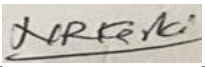

Prof. Dr. Nava Raj Karki

Program Coordinator

M.Sc. in Power System Engineering

Assoc. Prof. Jeetendra Chaudhary	Assist. Prof. Akhileshwar Mishra
Supervisor	Supervisor & DHoD
Department of Electrical Engineering	Department of Electrical Engineering
Assoc. Prof. Dr. Sujan Adhikari	Assoc. Prof. Mahammad Badrudoza
External Examiner	Head of Department
Pokhara university	Department of Electrical Engineering

Date: September ,2022

ABSTRACT

Grid losses and carbon impact are reduced by integrating renewable energy sources (wind and photovoltaic) into electricity networks. The intermittent nature of RES, however, greatly diminishes system inertia, which has an impact on the system's ability to dampen and modulate primary frequency regulation. Increased PV penetration may result in induced frequency oscillations that may go against grid operating standards and jeopardize the grid's stability and security. In this thesis, to decrease frequency oscillation by improving primary frequency controllability in accordance with grid code and enable more PV penetration, a Battery Energy Storage System (BESS) with droop control is suggested. The primary idea of BESS control is to mimic the governor's drooping behavior found in conventional generators. Fossil fuel based conventional producing unit replacement and the consequences of PV integration at various level with line & load contingencies is investigated. The optimal Sizing and location is also achieved through scenario and comparative performance analysis in this research. Theoretically sizing of BESS is done using inertia constant and droop control for 150 MW replacement of conventional generation with PV, 75 MW sizing of BESS is obtained. When a 100 MW of PV is penetrated with temporary and permanent line outage and heavy load, it is observed that frequency of grid is violated i.e. the frequency deviation of G1 & G2 are extremely oscillatory and exceed the required grid limit by 1.0204 (51.02 Hz; G1) and 1.0246pu (51.23 Hz; G2) respectively. With the addition of 50 MW BESS at bus 7 of IEEE 9 bus system, the frequency of G1 and G2 are under NEM 2% grid criteria i.e. 50.365 Hz & 50.487 respectively. Also for IEEE 14 bus system frequency rise violating the grid criteria with frequency 51.5 Hz with 140 MW PV penetration. The frequency observed with 100 MW size of BESS installed at bus 6 is 0.996 pu i.e. 49.8 Hz for both generators and oscillations are also minimized. RMS/EMT simulations are done for all scenarios in Dig silent power factory environment.

ACKNOWLEDGEMENT

I would like to express my immense gratitude to my respected supervisors Assoc. Prof. Jeetendra Chaudhary, Department of Electrical Engineering, IOE Pulchowk Campus & Deputy Head of Department Akhileshwar Mishra for their patience, motivation and continuous support in this thesis work. I could not have imagined a better advisor and mentor. Their suggestions, instructive guidelines and cooperative supervision have been motivating factors for me to pursue research activities with a proper target.

I am highly indebted to our program coordinator Prof. Dr. Nava Raj Karki, Department of Electrical Engineering, IOE Pulchowk Campus, for his insightful and flabbergasting suggestions and feedbacks. Also, I would like to thank the IEEE PES Nepal Chapter & Organizers of RESSD 2022 for providing me with the chance to publish my thesis work as a part of M.Sc. in Power System Engineering.

I would like to express my due respect to Associate Prof. Mahammad Badrudoza, Head of Electrical Engineering Department for his valuable and kind support. Also, I am extremely grateful to Assistant Prof. Dr. Samundra Gurung, Kathmandu University (KU) for his kind suggestions to this thesis works. Last but not the least, I extend my special thanks to my friends and families for their invaluable support and co-operation.

TABLE OF CONTENTS

COPYRIGHT ..... **iii**

ABSTRACT ..... **v**

ACKNOWLEDGEMENT ..... **vi**

LIST OF FIGURES ..... **x**

LIST OF TABLES ..... **xiii**

LIST OF ACRONYMS AND ABBREVIATIONS ..... **xiv**

LIST OF PUBLICATIONS ..... **xvi**

CHAPTER ONE. INTRODUCTION **1**

1.1 Background 1

1.2 Problem Statement 4

1.3 Scope…….. 5

1.4 Objectives 5

1.5 Thesis Organization 6

CHAPTER TWO. LITERATURE REVIEW **8**

2.1 Introduction 8

2.2 Frequency Stability 14

2.3 BESS Technology and Batteries 15

2.3.1 BESS Configuration Methods 17

2.3.2 Power Conversion System and Converter Technologies 19

2.3.3 SOC calculation of Battery 21

2.3.4 Battery Types 22

2.4 Application of BESS in RES 24

2.4.1 Output power smoothing/Load levelling 25
2.4.2 Frequency Regulation 25
2.4.3 Voltage Regulation 27
2.4.4 Important conclusions of BESS implementation 28
2.4.5 Major difficulties of BESS implementation 29
2.5 Charge/Discharge Cycle and Battery Lifetime 30
2.6 Sizing of BESS 32
CHAPTER THREE. METHODOLOGY 34
3.1 Frequency Control with PV and NEM Grid Conditions 34
3.2 Voltage and frequency control using the overall BESS modeling 35
3.2.1 Frequency Controller 37
3.2.2 Voltage Controller: 39
3.2.3 Active/Reactive power(PQ)controller: 40
3.2.4 BESS charge control and Charging management 41
3.2.5 Dq current controller 43
3.2.6 Sample Battery 44
3.2.7 Photo-voltaic (PV) 45
3.3 ATTRIBUTE OF THE TEST SYSTEM AND CASE STUDIES 46
3.3.1 Attribute of the test system 46
3.3.2 Low and Heavy Load scenarios 48
3.3.3 Scenarios Considered 49
CHAPTER FOUR. RESULT AND DISCUSSION 50
4.1 Modified IEEE 9 Bus System 50

4.1.1 Light load and generator control during a line event 51
4.1.2 Heavy load and both temporary and permanent line outages 53
4.1.3 BESS installation location & sizing 57
4.1.4 BESS Recharging 59
4.2 Modified IEEE 14 Bus System 59
4.2.1 Light load and generator control during a line event 60
4.2.2 Heavy load and both temporary and permanent line outages 63
4.2.3 BESS installation location & sizing 66
4.2.4 BESS Recharging 68
CHAPTER FIVE. CONCLUSIONS AND RECOMMENDATIONS 69
5.1 Conclusions 69
5.2 Recommendations 70
REFERENCES 71
APPENDIX A: System Model in Power Factory 77
APPENDIX B: Data of Modified IEEE 9 & 14 bus systems 88

LIST OF FIGURES

Figure 1.1: Complete thesis outline 7

Figure 2.1:Classification of Energy Storage technologies 13

Figure 2.2: European network of TSO defined frequency stages [7] 15

Figure 2.3: Application of BESS in RES Integrated System 16

Figure 2.4: Diagram of BESS connection in a PV/BESS Case; (a) An converter for PV/BESS Connection (b) Using DC-DC converter from common DC side for BESS(c) BESS directly connected on DC side 18

Figure 2.5: BESS diagram for PV-Wind-BESS ; (a) connecting through single DC bus (b) connecting through single ac bus [2] 19

Figure 2.6: BESS Operation modes [2] 20

Figure 2.7: parts of a Pb-acid Cell [15] 23

Figure 2.8: Components of Li-ion Battery [15] 24

Figure 2.9: Regulating voltage by implementing BESS [3] 28

Figure 3.1: Frequency regulation of PV integrated system using BESS [30] 35

Figure 3.2: The model of BESS in Dig SILENT/Power Factory 36

Figure 3.3: Primary frequency control with BESS [5] 37

Figure 3.4: Frequency and active power control of BESS [31] 38

Figure 3.5: p-f droop chac [3] 39

Figure 3.6: Voltage and reactive power control of BESS [5] 40

Figure 3.7:Voltage droop characteristics [5] 40

Figure 3.8: Charge controller ,d & q-axis controller [3] 41

Figure 3.9: The WSCC system with PV & BESS location [36] 46
Figure 3.10 : Modified IEEE 14 bus system network [34] 47
Figure 4.1: IEEE 9 bus system in Power Factory 50
Figure 4.2: The frequency of G2 (pu) for various Scenarios 51
Figure 4.3: The frequency of G1 (pu) for various Scenarios 52
Figure 4.4: Active power output(MW) of G2 53
Figure 4.5: Voltage at BESS connection point 54
Figure 4.6: Voltage [pu] for different scenario 55
Figure 4.7: Voltage [pu] for different scenario 55
Figure 4.8: BESS active and reactive power 56
Figure 4.9: Rotor angle plot of G2 for various BESS location 58
Figure 4.10: frequency plot of G2 for various BESS location 58
Figure 4.11: Battery recharging scenarios 59
Figure 4.12: Modified IEEE 14 bus system 59
Figure 4.13: Scenario 1 plot for speed and rotor angle 60
Figure 4.14: Scenario 1 Frequency plot for all gen 61
Figure 4.15: Scenario 1 Voltage plot for all gen 61
Figure 4.16:Frequency plot for scenario 2 62
Figure 4.17: Voltage plot for scenario2 62
Figure 4.18: frequency(pu) of G1 & G6 63
Figure 4.19: Voltage(pu) of G1 & G6 63
Figure 4.20 : frequency(pu) response with both PV & BESS 64
Figure 4.21: Voltage(pu) response with both PV & BESS 64

Figure 4.22:Active power o/p of G1 65

Figure 4.23:BESS Connection point voltage at different scenario 65

Figure 4.24: Frequency (pu)of G6 for different scenarios 66

Figure 4.25: Rotor angle plot for various BESS location 67

Figure 4.26: frequency plot for various BESS location 67

Figure 4.27 : SOC of Battery ;Active (MW)& reactive power(Mvar) provided by BESS Converter during contingencies 68

Figure A.1: The whole system model in Power factory 77

Figure A.2: Schematic diagram of BESS frame 78

Figure A.3 :Schematic diagram of Frequency Controller 79

Figure A.4: Schematic for PQ model 80

Figure A.5 : Charge control model 81

Figure A.6: Battery model 82

Figure A.7: PV system model frame 85

LIST OF TABLES

Table 3.1: Battery settings 44

Table 3.2: Load profile (MW) in Different Operation Modes 48

Table 3.3: Gen output at different operating strategy 48

Table 4.1: Various scenario & network contingencies and their impact on frequency 52

Table A.1: PQ controller settings 80

Table A.2: Charging control 82

Table A.3 : Battery parameters 83

Table A.4: BESS controller settings 83

Table A.5: PV array settings 85

Table A.6: Controller settings 86

Table B.1: Generator data for IEEE 9 bus system 88

Table B.2: Network Data for IEEE 9 bus system 89

Table B.3: Generator data for IEEE 14 bus system 89

Table B.4: Data of transformers based on 100 MVA 90

Table B.5: Data of lines based on 100 MVA 90

LIST OF ACRONYMS AND ABBREVIATIONS

AEMO = Australian Energy Market Operator

BESS = Battery Energy Storage System

CD = Conventional Droop

CDFP = Conventional Droop with the Proposed FLC Pitch Control

CDPP = Conventional Droop with PI Pitch Control

DFIG = Doubly Fed Induction Generator (DFIG)

DOD = Depth-of-Discharge

FACTS = Flexible AC Transmission System

FLC = Fuzzy Logic Controller

FRT = Fault Ride Through

LiFePO4 = Lithium Iron Phosphate

MG = Micro grid

MPPT = Maximum Power Point Tracking

NEM = National Electricity Market

NOFB = Non-Operating Frequency Boundary

P = Proportional

PEC = Power Electronic Converter

PCC = Point of Common Coupling

PCS = Power Conversion System

PFC = Primary frequency Control

PI = Proportional-Integral

PID = Proportional-Integral-Derivative

PLL = Phase-Locked-Loop

PSS = Power System Stabilizer

PV = Photovoltaic

PWM = Pulse Width Modulation

RES = Renewable Energy Sources

ROCOF = Rate-of-Change-of-Frequency

ROCOP = Rate of Change of Power

SGs = Synchronous Generators

SOC = State of Charge

SOH = State-of-Health

STATCOM = Static compensator

VRB = Vanadium Redox Battery

VSC = Voltage Source Converter

LIST OF PUBLICATIONS

Paper 1

A. K. Jha, A. Mishra, J. Chaudhary, “Battery Energy Storage System for Reducing the Impact of PV penetration on Frequency Regulation”, International Conference on Role of Energy for Sustainable Social Development, 8th-9th August 2022, Bhaktapur, Nepal

CHAPTER ONE. INTRODUCTION

1.1 Background

The integration of green and carbon free energy resources, particularly solar (PV) and wind energy, into the current grid is being driven by the continuous grow in energy consumption & increasing environmental concerns of conventional electricity production [1]. Government policies, societal movements, improvements in renewable energy technology, current installation scenarios, and research portfolios from academia and business all point to a power sector that will be emission-free in the future. As a result of such resolutions a same rate of RES penetration is anticipated in coming years too. Regarding the subject matter of this paper, adding large-scale RES of an alternating nature has created new difficulties for the dynamic and transient stability of the current electric grid. The operation of power systems has become more difficult because to RES, which have differing natures of operational traits in comparison to traditional generation units, as well as inherent swinging behavior. Additionally, as RES become more prevalent, the primary electric grid has a number of technical issues, including voltage limit violations, transmission bottlenecks, peak generation-peak demand imbalances, an increased requirement for load-generation balancing (spinning reserves), etc. Additionally, there is growing worry about how poor inertial RES penetration affects the system's inertial capacity, particularly with regard to how they affect the dampening of power oscillations after disturbances. In light of this, RES can deliver clean energy at the cost of stability anxiety. The goal would be to use as much renewable energy as feasible to generate electricity while minimizing risks to the power system's stability and dependability. In many nations, it is customary to use power electronics devices to improve power system stability and enable larger throughputs of renewable energy, primarily through the use of various energy storage technologies. An energy storage system's power electronics technology advancements have the capacity to react quickly. The current electric grid, which now includes RES, confronts several technological obstacles that have yet to be overcome. In order to reduce the negative effects of RES, significant efforts have been made to simulate energy storage systems for utility-scale power system modeling. Battery Energy Storage System (BESS), one of several

energy storage technologies, has been utilized to address the issues associated with a large penetration of RES in the electric power grid by improving power system stability [2]. BESS is leading the way primarily as a result of recent technology advancements and falling battery prices. Additionally, a BESS can now provide more services than in previous decades. In order to support transient stability and increase the penetration of RES in the current electric grid, this study effort improves the area of BESS application on the grid level. This study focuses on the comprehensive modeling of BESS with distinct active and reactive power regulation mechanisms. Maximizing BESS power is of utmost relevance when considering transient stability support.

As long as the power electronics converters and transformers are appropriate, the BESS may be connected to the power system at any voltage level. A BESS can offer both technical and financial advantages, such as the ability to control the frequency of the power system by regulating the rate at which the battery is charged and discharged, reduce transmission congestion, which is advantageous for utility companies, lower costs for customers, and compensate peak time generators, which lowers the cost of electricity generation.

BESS is becoming more and more common as a result of batteries' quick technical advancements. The Li-ion battery made its debut on the market in 1991, and because to their better energy density, minimal maintenance requirements, and low self-discharge, they quickly gained popularity. Despite having concerns with protection, temperature, environment, and fragility.

It illustrates how PV penetration affects primary frequency control damping performance in the power system. More crucially, it is shown when, as PV penetration rises, the electric system no longer complies with grid standards. In order to estimate network operating state for evaluating PV penetration, particular emphasis is given to production control & system loading, both of which have a substantial impact on the transient nature of the grid. BESS is introduced to increase the system's primary frequency controllability and give more system dampening [3]. In addition, with the expansion of PV penetration, the impact of the generator's control and system loads on the grid's damping performance is further

examined. Results from the simulation show that BESS effectively enhances the system's capacity to dampen in response to primary frequency control contingencies. BESS thereby helps to provide for rising PV growth in the electric grid and decreases inertia-related challenges with higher PV penetration.

1.2 Problem Statement

Due to their degree of grid penetration, PV received less attention than wind generation. However, it is anticipated that PV penetration would expand from its current installation scale by around 59.6% by 2022, mostly as a result of decreased pricing for technology associated to PV generating. Therefore, it is now necessary to conduct a detailed analysis of the impact of PV penetration and take into account the dynamic influence of PV. Since a PV system has no moving elements, unlike a wind turbine, there is no kinetic energy that may be stored and utilized in the event of a contingency, most notably an under-frequency occurrence. As a result, PV penetration will drastically reduce system inertia, which might cause serious concerns about the grid's stability. Reduced inertia, according to several research studies, raises the grid's frequency deviation. The increased penetration of PV might cause frequency oscillations that may violate grid operating specifications and endanger the grid's security and stability.

1.3 Scope

- In order to ensure that BESS is used to its fullest potential while still providing the essential services, battery size and placement are very important. Therefore, to find the best size and location of BESS installation for maximal techno-economic value, optimization methodologies including “stochastic, heuristic/meta-heuristic, and evolutionary computing techniques” might be applied.
- The ideal parameter tuning of the BESS and the adaptive droop parameters has to be carefully considered in order to improve the ability of the BESS and the wind turbine/PV module to respond to changing operating circumstances.
- Considering the widespread use of artificial intelligence and machine learning algorithms, these techniques may be further incorporated for controlling BESS.
- Future research will pay more attention to techno-economic assessment through optimization during grid service.

1.4 Objectives

The main objectives are summarized as follows:

- The primary work is to design & develop a BESS model that is suited for Frequency regulation of grid.
- To enable greater penetration of PV energy into the current electric grid while taking transient stability issues into consideration

1.5 Thesis Organization

The thesis works contains total of five chapters and each chapter contains the following: Chapter 1 discusses the purpose of the study, the goals of the research, and the novel scientific contributions. This chapter also highlights the whole thesis outline and provides a synopsis of each chapter. The statement of the problem, various objective and scope are also highlighted.

Chapter 2 focuses on the literature that this thesis works gone through. Also provide brief introduction of Renewable Energy Sources, Ancillary Services, Battery Energy Storage System, power Electronic Converters and different scenario overviews.

Chapter 3 details explains the methodology to achieve the proposed objectives. It exemplifies how PV penetration affects the effectiveness of damping in the primary frequency control mechanism. More crucially, it is shown when, as PV penetration rises, the electric system no longer complies with grid standards. BESS is used to increase the system's primary frequency controllability and give more system dampening. In addition, with the expansion of PV penetration, the impact of the generator's control and system loads on the grid's damping performance is further examined.

Chapter 4 presented the results and discussions of the proposed mechanism in various case scenario. The simulation findings show that BESS effectively enhances the system's capacity to dampen in response to primary frequency control contingencies. BESS thereby helps to provide for rising PV development in the electric grid and decreases inertia-related challenges with higher PV penetration.

Chapter 5 presents future work domain based on the findings in this work and summarizes main conclusions of the work.

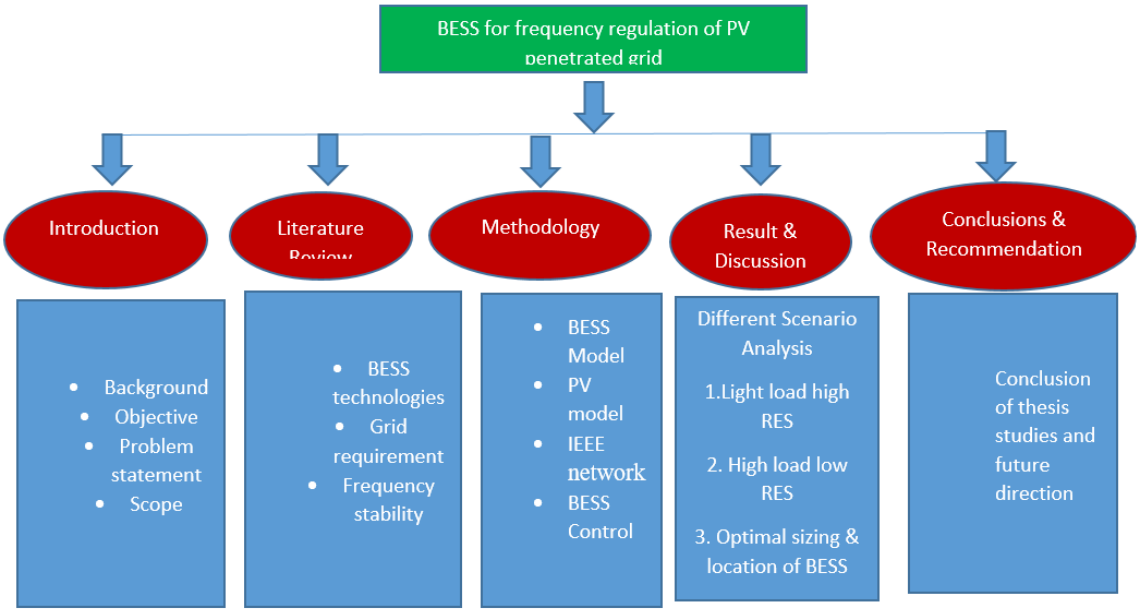

Figure 1.1: Complete thesis outline

CHAPTER TWO. LITERATURE REVIEW

2.1 Introduction

The rapid growth in energy demand & sustainability concern of conventional generation push the energy world towards RES (PV & Wind). The grid experiences problems as a result of high RES penetration, including voltage limit violations, transmission bottlenecks, gen-demand imbalances, and a higher need for spinning reserve due to either poor inertia contribution from the high renewable energy resources or replacement of convention production unit within the grid [1]. Due to greater RES penetration in electric power systems, the power system's dynamic and transient stability performance is being negatively impacted by the decreased system inertia and the drop in reserve capacity. Even system may collapse “a complete blackout” in extreme case due to more stress on grid caused by higher RES penetration [2]. Due to their low degree of penetration, the dynamic impact of PV energy systems has not previously been studied. Reduced available inertia caused by increased PV capacity might have a detrimental impact on the system's dynamic and transient stability. Therefore, detailed impact of PV is need to be completely studied.

Energy storage devices can control its output, reducing the negative effects of RES indeterminacy. One of the most promising technologies, BESS has the ability to independently manage both active and reactive power. The BESS structures typically include a transformer, a power conversion system, and a battery bank. BESS can be used to absorb extra solar energy produced during peak generation, reducing the effect of solar on the voltage rise of the grid. During charging the power flow direction of BESS is negative and vice versa. The SOC of battery is simply battery capacity that can participate in charging and discharging. The latest fast charging technologies, lowering market price, high energy density make the Li-ion batteries popular for BESS applications [3].

Many scenarios with different level of PV penetration following transient events are analyzed in this paper that may have severe impact on the system’s grid frequency control which keeps frequency oscillation within the minimum grid standards. In order to improve the system's capacity to dampen oscillations and manage the output response of the system

within grid-defined constraints, a droop-controlled BESS is presented. Many study cases are executed to present the effectiveness of BESS in minimizing the negative impact of greater PV penetration. Additionally, system loads and conventional generator control dominance on primary frequency response with greater PV penetration are both investigated.

Paper [4] illustrates how a separate MG may be controlled in terms of frequency by using DFIG-based wind turbine regulation. For controlling system frequency, sectional droop and inertia emulation are controlled in concert with PI & fuzzy logic controller (FLC). OPAL-RT is used to run the simulation in real-time.

Paper [2] compares the power grid's dampening performance for various levels of wind energy penetration to that for no wind energy. BESS is included into the network to increase system damping capacity. The effectiveness of BESS is shown to boost the system's capacity to dampen vibrations and reduce over- or under-frequency excursion brought on by unexpected occurrences with greater wind energy penetration. It is demonstrated that the inertial effects of higher wind energy penetration may be reduced when BESS is used in the grid.

The effect of Photo-voltaic injection on power grid dampening outcome in grid frequency regulation is shown in Paper [3]. More crucially, it is shown when, as PV penetration rises, the electric system no longer complies with grid standards. In order to estimate network operating state for evaluating PV penetration, particular emphasis is given to control of production & loading, both of which have a substantial impact on the transient nature of the grid network. BESS is used to increase the system's primary frequency controllability and give more system dampening. In addition, with the expansion of PV penetration, the impact of the generator's control and system loads on the grid's damping performance is further examined. Simulation findings show that BESS effectively enhances the system's ability to dampen responses. BESS thereby helps to provide for rising PV development in the electric grid and decreases inertia-related challenges with higher PV penetration. Simulations are used to support the suggested SOC recovery strategy's effectiveness.

The application of Stat-Com & BESS in increasing the transient performance of a huge grid & expanding the capacity of power export within two equally large interconnected power systems is demonstrated in Paper [5]. “In the future electric grid, where aging transmission lines, intermittent RES, and a complicated electricity market are the key determinants of power system stability, STATCOM and BESS technologies are at the forefront. Different single/multiple network/load events are applied when exporting electricity in an analogous transmission network to show how well they function in comparison. A few additional network events are also taken into consideration to demonstrate the effectiveness of BESS and STATCOM. It has been proven through simulation tests that STATCOM cannot keep voltage and frequency stability when the system is exporting 44% more than its typical working limit and runs into persistent network problems. However, the integrated BESS provides the system with the necessary damping and is capable of withstanding single/multiple network/load contingencies, transient single-phase-to-ground faults, and permanent ones.”

The potential of BESS to lessen transformer overloading and increase the capacity of the charging station is demonstrated in Paper [6]. Using a mechanism controlled by real power feedback, BESS modeling is created. BESS is also intended to provide grid services and

smooth out PV. Simulated experiments are conducted to confirm BESS effectiveness at the planned charging station.

Power system reliability and security issues arise as a result of the widespread addition of RES in place of conventional power plants (CPPs). The goal of this study is to enhance the grid's frequency response following a contingency event in power systems with significant wind power penetration. An energy storage system (ESS) might be a viable solution for providing inertial response and primary frequency regulation. Here, a method for sizing the ESS in terms of needed power and energy is presented. It defines the contribution of the ESS to the grid, in terms of inertial constant and droop. The concept is introduced to a 12-bus grid network with substantial wind power penetration [7].

All the above papers describe the various application, sizing and modelling of BESS and there are many papers attached in reference regarding the Dig silent power factory, grid criteria and system considered here.

In future power systems with a large penetration of renewable energy sources, energy storage (ES) technologies paired with a control strategy are among the promising options to reduce these frequency stability difficulties. Energy storage will assist in managing the erratic output from RES, and it will also require a control system to best balance supply and demand. However, in this instance, the energy storage system (ESS) can be characterized as a technological device interfaced to the grid to store the surplus electric power by charging during overproduction and then delivering the stored electric power back by discharging during power shortfall. Different categories have been created for the ES technology as shown in figure 2.1.

Pumped storage hydropower: is a mechanical energy storage device with the ability to store the largest amount of energy capacity by this time. The working principle of this device is based on two reservoirs of water placed on different height levels. Using the extra electric power, water is pumped from the lower reservoir to the upper reservoir, storing the energy. On the hand, the power generation happens when the water falls from the top to lower reservoir.

• Compressed air-energy storage: This type of storage device performs its task using the gas turbine. It stores the energy through compressing the air into the chamber using the surplus power. Then the electricity is generated by releasing the air through the turbine during the power deficit.

• Flywheels: The flywheel devices perform the storage task through motor-generator compound. This converts the energy into rotational inertia during overproduction, and this is later extracted to provide the power during overload.

• Battery energy storage: This device consists of electrochemical cells through which the electrical energy is stored in form of chemical reactions using the surplus power, and this is later converted back to electricity during power deficit.

• Thermal energy storage: This device stores the electrical energy in form of heat from the surplus electric power. The stored heat can either be used to provide heating or converter back to electric power.

• Super-capacitors: These store the electrical energy in form of electrostatic charge. These devices provide high fast response to the power demand, but can only supply less amount power compared to most other storage technologies.

• Hydrogen storage: The energy is stored in chemical reaction, where the hydrogen can be obtained from water through electrolysis process and the surplus electrical power

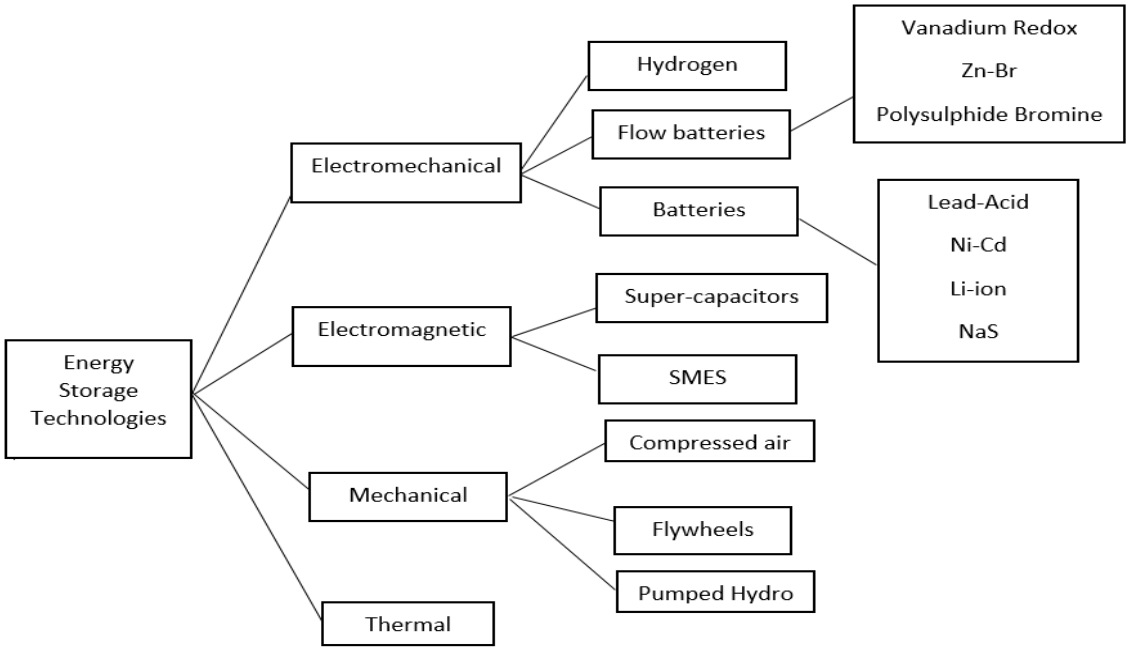

Figure 2.1:Classification of Energy Storage technologies

The BESS has many advantages over other energy storage technologies, including cost effectiveness, safety, and flexibility because it can be installed anywhere, unlike compressed air and pumped hydro storage, which call for sizable underground air reservoirs and water tanks, respectively. The BESS will be employed in this project to provide frequency stability in the system with variable power from RES.

2.2 Frequency Stability

For a power grid to be stable and reliable, the frequency needs to be kept almost constant. This is accomplished by maintaining the system's active power balance utilizing a variety of control reserves, some of which are built into the synchronous machine and others of which are supplied by the central control hub. The following is a description of the typical frequency control methods:

• Inertial control reserve: This type of control reserve is inherently provided by the synchronous machine using the kinetic energy that is stored in the rotating masses of machine, that is later released when the frequency deviates from the nominal value.

• Primary control reserve: This control reserve is automatically executed by a speed governor that senses the speed change of generator due to change in load, and then adjust the output power of generator.

• Secondary control reserve: This control is automatically activated after the primary control fails to return the frequency back to the nominal magnitude. In this control method, the frequency deviation is normalized using a PI type-controller, and is expected to operate within 30 [s]-15 [min] after disturbance occurrence

• Tertiary control reserve: This is manually activated to support the secondary control during a large disturbance in the system. The tertiary reserve occurs by using economic dispatch of generation, and is expected to operate within 15-60 [min].

The classical power system, which is predominately made up of large-scale synchronous generators, is frequently suitable with the control methods outlined above. But when converter-based generation sources like WTs and PVs increasingly take the place of synchronous generating units in the modern power system, the system's inertia degrades, making the frequency of the system more susceptible to disruptions. As a result, new solutions are required to address the stability issues in this scenario in order to maintain a sustainable power supply despite the rise of RESs. The BESS is one of the potential options

and is growing in popularity and integration into the power grid as a result of its many benefits, particularly with regard to system frequency stability.

Large synchronous generators (SGs) typically handle short-term power imbalances and keep the grid frequency constant. According to their droop settings and available capacity, SGs can respond to inertia caused by the machine's physical inertia and then perform primary, secondary, and tertiary frequency control as shown in Figure 2.2.

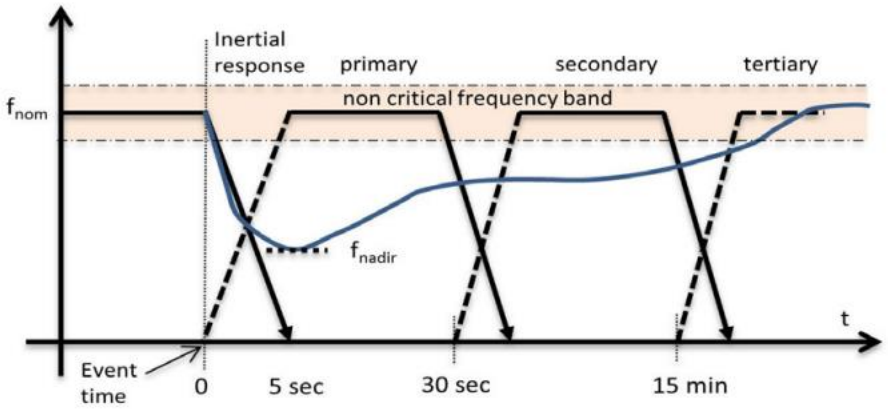

Figure 2.2: European network of TSO defined frequency stages [7]

2.3 BESS Technology and Batteries

Due to its capacity to provide operational flexibility, quick reaction, decrease in price/kWh [8] and scientific improvement in modern battery technologies, battery technologies are becoming more and more common in power system applications. Batteries are often employed in power systems at all voltage levels [9]. Utilizing them can guarantee operational flexibility and environmental advantages. The poor energy density and power capacity of battery storage devices, however, prevent their widespread usage in large-scale applications. However, recent developments in battery technology, particularly with regard to lithium-ion batteries, have stoked interest in their use in massive power systems.

Energy storage systems can control their output, reducing the negative effects of RES inconsistency. The “flywheel, pump hydro, capacitor, super-capacitor, and compressed air energy storage” are only a few of the available energy storage technologies. BESS gives superior adaptability in terms of size and location & quick reaction to meet the needs for application of storage system [1]. As illustrated in Fig. 2.3, BESS offers a variety of services, including energy storage, autonomous regulation of real & virtual power flow at the common coupling point, and service delivery. Transient frequency stability, increased reliability, peak shaving, management of transmission congestion, output power leveling, ramp rate control, and dispatchability are a few possible BESS services. Regulating the BESS active power output can enhance plant dispatchability, frequency management, peak shaving, and output power fluctuation mitigation. On the other hand, by controlling BESS reactive power, voltage management, & poor voltage ride-through may be achieved.

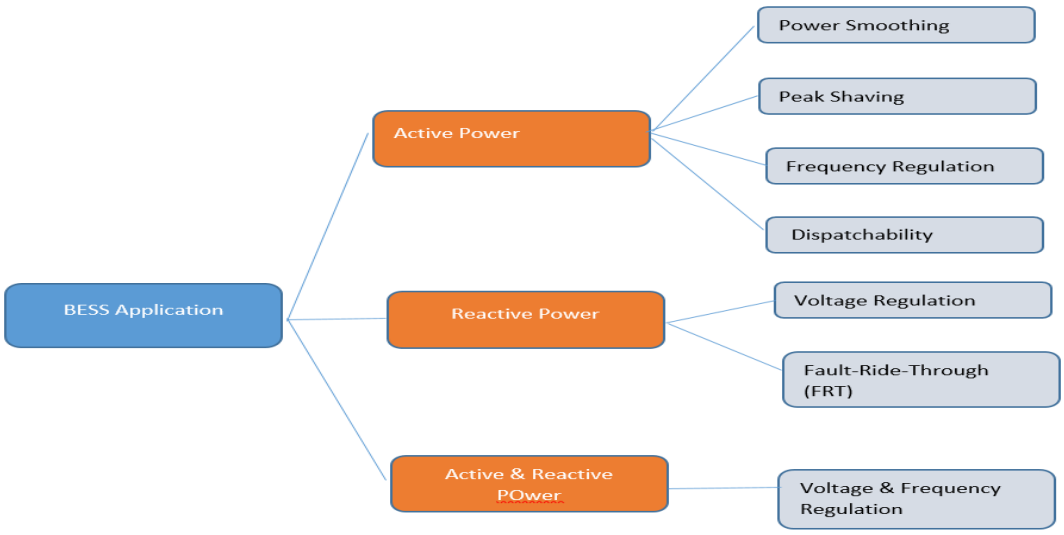

Figure 2.3: Application of BESS in RES Integrated System

2.3.1 BESS Configuration Methods

The voltage level at which BESS is designed to be linked largely determines its fundamental structure. Battery banks, which are generally parallel battery packs, and a DC to AC inverting arrangement might make up a typical BESS model. A transformer could be needed to convert the output voltage level of the BESS to the grid voltage level if it is planned for the BESS to be connected to a local distribution or transmission system. Very frequently, BESS obtains and distributes electricity through the grid, necessitating a bi-directional converter based on voltage source or current source, with its choice primarily relying on the function of BESS in that specific objective. Fig. 2.4 displays typical BESS-PV arrangements. Every setup has pros and cons of its own. Figure 2.4(a) illustrates how adding another DC/AC converter would raise system costs. Additionally, since BESS is connected to the PCC directly, a second circuit protection device is required, which drives up system costs even more. However, the main advantage is that BESS may be managed as a separate storage system for grid service. The intermediate DC-DC inverter with BESS in Figure 2.4(b) provides the flexibility to be linked with various DC-link voltage levels as it permits boosting the battery voltage to the high DC-link voltage. The DC-DC converter is not required according to the block diagram in Figure 2.4(c). Only a battery voltage equivalent to the DC-link voltage is appropriate for this system. Battery SOC changes for grid synchronization, and thus necessitates correct inverter management with the variable DC-link voltage because the battery cannot be regulated.

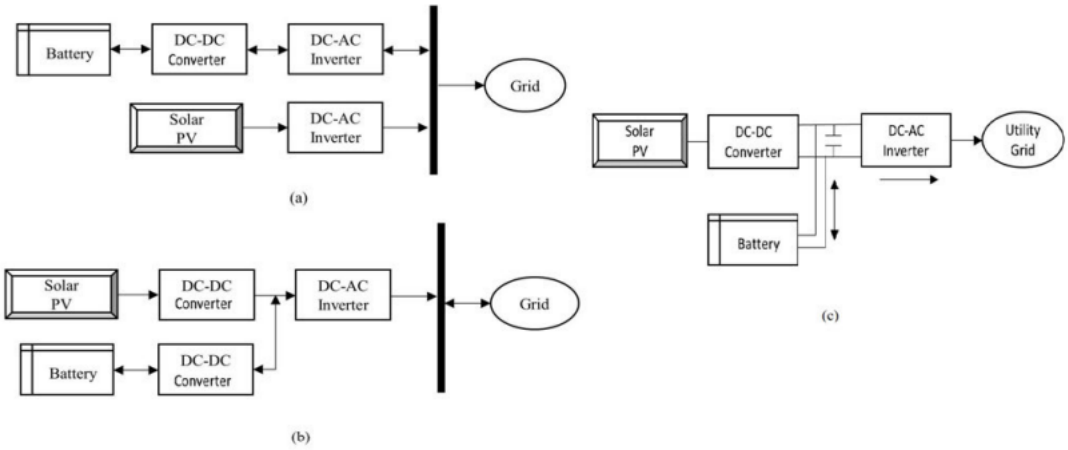

Figure 2.4: Diagram of BESS connection in a PV/BESS Case; (a) An converter for PV/BESS Connection (b) Using DC-DC converter from common DC side for BESS(c) BESS directly connected on DC side

Battery connections for a hybrid energy system can be made to either a DC or an AC bus, depending on the design constraints and preferences. The battery banks may be integrated into the DC bus directly or in conjunction with a DC-DC power conversion system. A battery bank with a DC/AC power conversion system that is connected via an AC bus is another alternative for the BESS connection. Before or after the local AC bus connects to

the grid, a transformer can be built at the BESS output. Figure 2.5 depicts a few feasible PV-wind-BESS topologies.

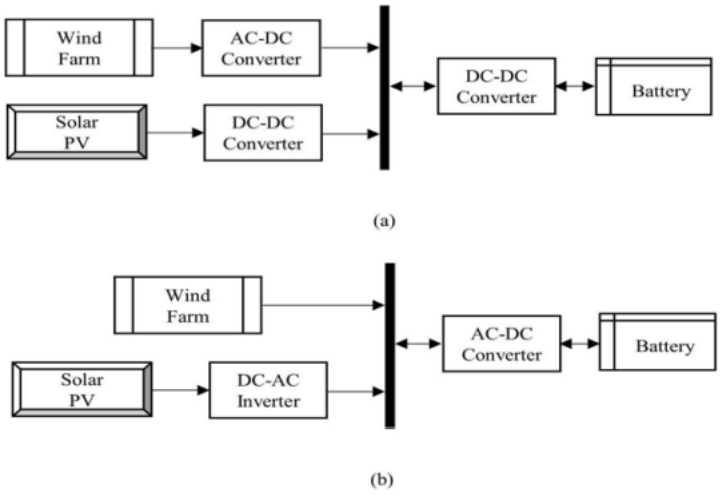

Figure 2.5: BESS diagram for PV-Wind-BESS ; (a) connecting through single DC bus (b) connecting through single ac bus [2]

2.3.2 Power Conversion System and Converter Technologies

A power electronics-based interface called a power conversion system (PCS) links a storage system to an AC power source. Due to the DC interface used by battery storage systems, batteries and PV's DC terminals can be combined and connected to the single dc bus. A wind farm terminal, however, does not provide such a prospect. Consequently, PCS is essential to link a BESS with the AC grid. As required by modern grid applications, PCS conducts both instantaneous real as well as virtual power management with high efficiency, quick response, and control design. Primary and secondary layer controls make up the PCS [10]. In order to regulate the power converter's power command and choose the best operating style on the basis of state of charge, energy tariffs, and system condition, main control creates gate drive signals. Active, reactive, and other data are sent to the secondary control.

The simplest main control strategy is proportional plus integral control. Secondary control chooses the power converters' operating style. There are three common techniques: - Charge mode - Discharge mode - Standby setting.

According to Figure 2.6, the direction of power flow indicates the output of the BESS, which is charging (negative) and discharging (positive). When everything is perfect, BESS output is 0. Because of battery self-discharge and converter loss, actual power flow in the BESS will be relatively low.

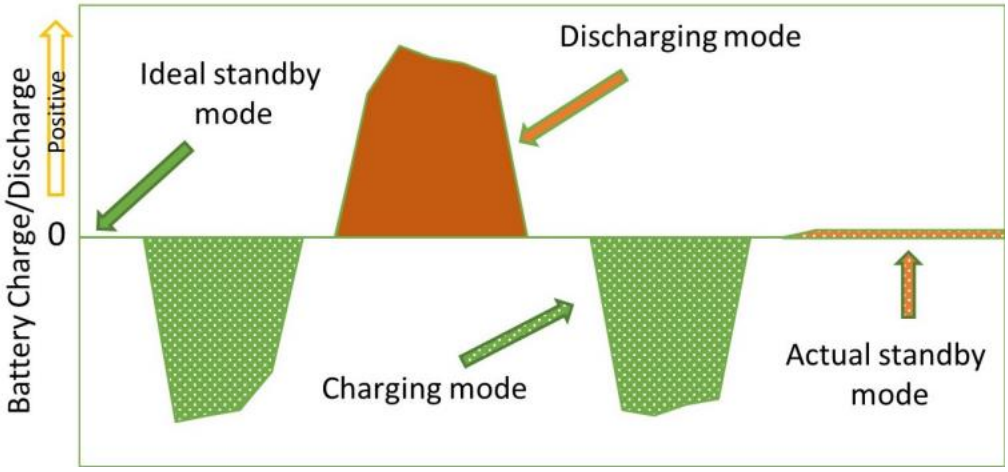

Figure 2.6: BESS Operation modes [2]

2.3.3 SOC calculation of Battery

As from perspective of power and energy use, the SOC is the cell capacity that is readily available to take part in charging/discharging cycles. The following measurable quantities are used to assess battery SOC:

- Cell/electrolyte Temperature
- Outside temperature
- Ampere-hour tally
- Age of batteries
- Battery voltage
- The electrolyte concentration.

The Coulomb Counting Method [3] and Open Circuit Voltage techniques are viable approaches to calculate a battery's state of charge (SOC), but their accuracy is questionable since it depends on the starting inaccuracy and cumulative noise in the voltage and current measurements. Another technique for calculating SOC is an "intelligent Recurrent Neural Networks (RNN) approach based on battery voltage/current and ambient temperature. However, RNN is a training-dependent approach, which may not perform well for untested data sets." Additionally, such that method skips the inner battery characteristics, the inaccuracy may continue to be present in SOC estimates. The closed loop technique of the model-based method, in contrast, makes use of estimate algorithms to routinely correct SOC error from measurements of voltage, current, and temperature in order to provide a SOC calculation that is more accurate. One of the most popular strategies for calculating SOC is a "dual fractional-order extended Kalman filter" or another kind of same. Numerous SOC calculation techniques have been successfully applied. The battery SOC can be calculated using equation (1):

$$\mathbf{SOC(k)} = SOC(k-1) + \int_{k-1}^{k} \frac{n.Ib}{3600\ Cb}\, dt \qquad \text{Equation (1)}$$

The BESS's DC terminal voltage is 0.9 kV. Each battery cell's maximum and minimum voltages are taken to be 13.8 volts and 12 volts, respectively. When completely charged,

sixty-five cells are connected along to create 0.9 kV. The BESS converter's AC terminal voltage is 0.4 kV. Through a 0.4/230kV transformer, BESS is integrated into the grid.

2.3.4 Battery Types

The most developed technique of chemical energy storage is rechargeable batteries, which are favored in power system applications [11]. Numerous electrochemical cells are connected in series or parallel in a battery depending on the required voltage and capacity [12]. Each cell has a positive electrode and a negative electrode that are separated by an electrolyte, which can be a paste, liquid, or solid. During charging and discharging, the conversion of chemical energy to electrical energy & vice versa should be energy-efficient processes that result in little physical changes. Rechargeable or secondary batteries have a rapid response time (s) [13], making BESS a well-liked and often utilized choice for improving steady-state and dynamic stability in power systems. For use in power system applications, batteries [14] [15] that have the following critical qualities or performance characteristics:

• Power and energy capacity;

• battery life span;

• battery efficiency;

• Temperature of the battery;

• State -of -charge;

• depth of discharge;

• Self-discharging;

• dimensioning;

• Requirements for care

Energy storage can last for hours or even months. The following subsections provide a quick overview of the various battery technologies employed in renewable energy systems.

2.3.4.1 Lead-acid Batteries

Lead-acid batteries have been the most advanced and widely used rechargeable battery technology in power systems since they first saw widespread use in 1860. As illustrated in Figure 2.7, a Pb-acid cell consists of a PbO_2 positive electrode and a sponge Pb^{--} electrode that are separated by a microporous material [16]. Its 5- to 15-year life cycle restricts its use for large-scale storage notwithstanding its 70–90% efficiency. The most popular lead-acid battery types are valve-regulated (VRLA) and flooded batteries.

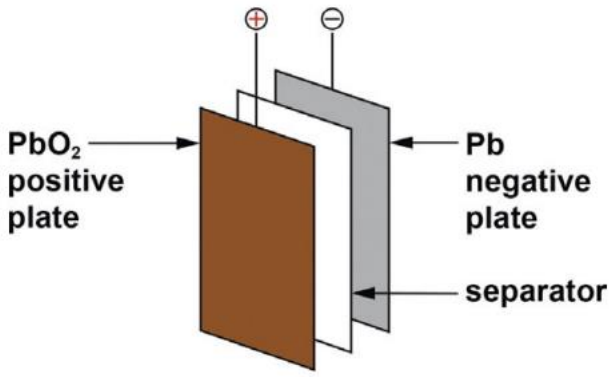

Figure 2.7: parts of a Pb-acid Cell [15]

2.3.4.2 Li-ion batteries

With over 50 years of technological advancement, Li-ion batteries are widely used in power grid applications and hybrid electric or plug-in hybrid vehicles [17]. Lithium-ion batteries have an anode made of lithiated graphite or lithium titanate and a cathode made of lithium metal oxide or a lithium metal phosphate, which are separated by an electrolyte composed of lithium salts, as shown in Figure 2.8. The higher capital cos $/kilowatt-hour is the issue with this type of battery. Lithium iron phosphate (LiFePO4) produces an orthorhombic olivine-like structure with somewhat deformed O2 atoms. Despite having a lower energy density, it exhibits less heat production. The most valuable material for use in electric vehicle (EV) applications is LiFePO4. Electrodes are isolated from one another in Li-ion polymer batteries by microporous poly-olefin. Because of their greater power and

energy density and less memory effect, these batteries are becoming increasingly appealing for use in EVs and renewable energy sources [18].

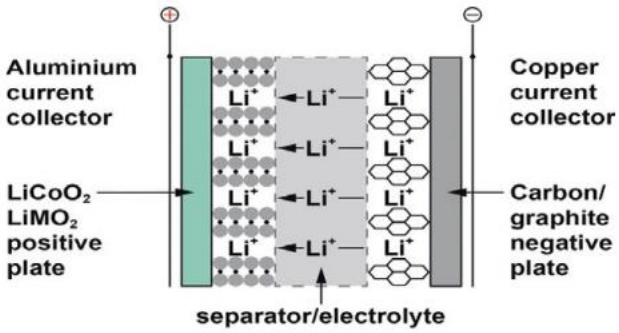

Figure 2.8: Components of Li-ion Battery [15]

2.4 Application of BESS in RES

BESS has been used in the electrical grid for several decades. However, BESS is quickly overtaking other energy storage technologies as one of the primary applications in contemporary power systems due to the increasing amount of intermittent RES penetration. BESS increases dependability and gives a wind/PV farm operational versatility. A hybrid model has attracted huge interest internationally recently due to their complementing behaviors. However, the steady functioning needs assistance from auxiliary energy sources regardless of whether the system is an interconnected system or a hybrid island system. This section analyzes and summarizes a thorough review of recent studies on various BESS implementation in RES integrated grid network.

2.4.1 Output power smoothing/Load levelling

Solar radiation, surrounding temperature, panel temperature, cloud cover, and operational parameters are the key factors influencing PV production. A steady power production from PV to the grid is always preferred, and it is definitely feasible to achieve this [19]. However, this may cause batteries to charge and discharge quickly, which would shorten their useful lives. The battery storage energy management technique occasionally enables the purchase and sale of electricity to the grid. The peak-to-mean ratio (PMR) is not decreased as a result, and an improved BESS Application in Renewable Energy System management approach is recommended in [20] that decreases peak-to-mean ratio. Moving estimation approach establishes the estimated generation of system, reduces storage capacity to offset error, and improves load supply. In contrast to ramp-rate control, this approach has a recall impact that causes frequently switching of BESS to produce greater energy losses, which shortens the battery life cycle. Longer window sizes lessen the shift in ramp/min, and the magnitude of the window size determines the level of smoothness (ramp-rate in Watt per minute). To even out PV power and satisfy the intended load demand, BESS runs in charging or discharging mode that depends on the excess or lack in solar output. The fact that BESS goes through a large number of charging/discharging cycles, which lowers a battery's lifespan, is one of the key disadvantages of this type of method.

2.4.2 Frequency Regulation

With a higher percentage of renewable energies, the inertia of the power system reduces reciprocally. As a result, renewable power facilities must correspondingly modify their output power to counteract frequency variation. Through PV curtailment, the PV controller may be used to offer frequency management for systems that are subject to over-frequency support [21]. It is feasible to implement under-frequency support, however doing so necessitates operating PV at a position different than the maximum power point (MPP) [22]. Due to the intermittent nature of PV production and its dependence on the weather, PV facilities must set up a dispatchable auxiliary energy supply to sustain system frequency as required. In a PV plant, batteries are a well-researched storage option to sustain system

frequency. Whenever there is a low PV output, electricity may be returned to the system and the battery can be charged at peak generation. Power fluctuation is lessened by battery storage, which also enables quick reaction to frequency variation [23]. Another option for frequency management is to use PV and BESS together, with BESS injecting active power when PV output is insufficient. Even though the power-frequency droop (P/f) characteristics specified in (2) might have either fixed or adaptive characteristics, an adaptive P-f exhibits smoother transitions under various management systems. Technically and financially challenging, coordinated optimum frequency regulation and self-consumption for battery recharging sometimes need a trade-off between them. The droop value R_{pf} in relation to variations in frequency (Δf) from the reference point, determines the degree of active power control of BESS (P).

$$\mathbf{P} = \frac{\Delta f}{Rpf} \qquad \text{Equation (2)}$$

BESS lowers frequency oscillation in addition to reducing frequency drops as compared to no BESS. Large-scale wind power plants are replacing conventional generators, therefore in the future, wind power facilities will need to start supporting frequency control. Inertial control [24] and pitch control provide proof that wind farms are involved in frequency management. High frequency support is primarily managed by battery charging and discharging in accordance and the pitch control mechanism for low frequency support. [25]. In cases of extreme under-frequency, battery Bess can sustain grid frequency on the basis of power mismatches. Battery storage allows for peak shaving, giving stored energy during the low wind period, and regulating system frequency. However, it is suggested that because a lot of power is needed quickly, coordinated control offers superior frequency management than individual BESS or wind turbine control. However, a coordinated control technique allows the wind farm to manage its production for regulating frequency, and battery storage will make up the difference if the requirement for regulation is not met. The efficient use of BESS enables reduction of unforeseen energy use, prevention of wind variations, and provision of extra regulation functions without lowering battery life. Extra

benefits and financial gains, however, are dependent on battery technology, market pricing, and wind power estimate accuracy.

The drawbacks of wind and PV are reliant on unpredictable air velocity and inconsistent sunlight. Because of their unpredictable behavior, green energy sources frequently have trouble meeting load demand, which has a significant impact on system frequency. In addition, the system may become unstable due to the hybrid power output's fast fluctuation. For long-term frequency regulation service, diesel generators can be employed to offer secondary frequency support in addition to Bess & PV for support of the main frequency. When generators produce low frequency oscillations to adjust frequency instead of high frequency oscillations, adaptive SOC can be implemented into the feedback control to reduce stress on the standard generators.

2.4.3 Voltage Regulation

Variable renewable energy generation must adhere to strict voltage management regulations in order to maintain nominal voltage within the working limit. When the voltage drops or rises, battery storage reacts swiftly by charging or discharging the battery and taking the initiative to keep the power system's voltage source constant. When there are little or no load demands during peak PV generating periods, there is a voltage spike that causes electricity to flow backward into the network. However, voltage violations may also be caused by a sizable dispersed generating unit at a single connection point. To counteract this unfavorable effect of significant PV penetration in low voltage distribution networks, a number of remedies have been put forth. One possible option is PV curtailment, although this will lower the maximum utilization of PV generation capacity, hence reducing the financial advantage. PV converter reactive power correction, voltage regulator installation, and transformer tap adjustment are further options that have been used. Another option to lessen feeder losses may be grid strengthening, although it is also more expensive. As illustrated in Figure 2.9, BESS may be utilized to consume excess PV energy during peak generation, minimizing the effect of PV on the grid's voltage rise. Depending on the requirements of the network, BESS can be built to manage virtual power or absorb excess to maintain grid voltage within the permitted range.

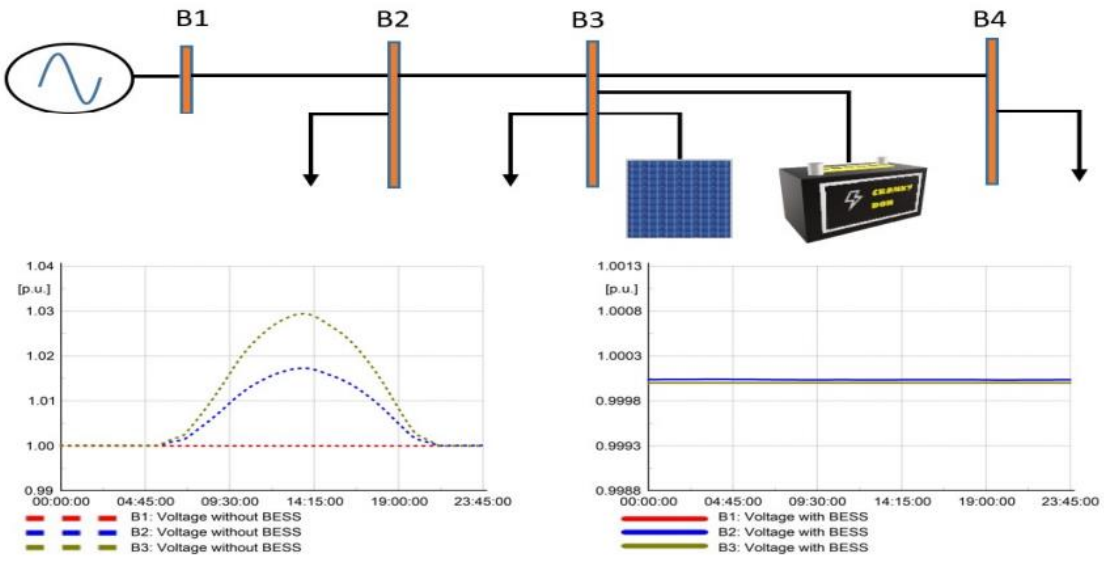

Figure 2.9: Regulating voltage by implementing BESS [3]

2.4.4 Important conclusions of BESS implementation

In order to offer the necessary real & virtual power support for renewable energy systems, a thorough assessment of the current literature reveals the significance of BESS implementation. These studies' main conclusion can be summed up as follows:

- Tracking output power is typically used as a reference to provide the damping of active power oscillation, and BESS provides the necessary power imbalances. Voltage, frequency or both may be employed as an error signal for BESS support in various Scenarios.
- The most prominent battery technologies are lithium-ion, lead-acid, sodium sulfur, and flow batteries due to their technical advancement and scalability in the MW range capacity.
- To prevent battery overcharging/discharging and detrimentally compromising battery longevity, it is essential to use SOC-based battery control design. High prediction inaccuracy, however, may make it difficult for the SOC feedback-based

control technique to maintain the necessary smoothing performance over an extended period of time.

2.4.5 Major difficulties of BESS implementation

An extensive analysis of BESS use in renewable energy systems indicates the efficiency of BESS components, possible installation issues, and energy control policy. The following is a summary of the major difficulties:

- The projected and actual production of RES power output differ significantly more in a day ahead market than an hour ahead market. Due to the promise for a significant BESS sizing in the 24 hour ahead market and the resulting rise in placing costs, participation in such a dispatchable market requires techno-economic feasibility.
- The installation cost of BESS is still fairly costly, which deters RES farm owners from using the technology. Therefore, a high-efficiency and cost-effective BESS technology is needed to reduce obstacles to BESS adoption.
- Power electronic converters (PECs) are used to link wind turbines and solar panels to the grid, therefore developing PEC control strategies may help with effective power management and lower converter losses.
- Battery power requirements are far more volatile than battery energy requirements, which complicates real-time BESS functioning.

- PI, Proportional (P), and Fuzzy Logic Controllers are the controllers utilized in BESS controls the most frequently. To determine the grid's output response, a comparative analysis of these available controllers or novel controller algorithms must be conducted.

- The effect of a battery storage system failure or other disturbance on the linked network is still under research.

- For a battery to have enough capacity to participate in the energy market or to improve stability, it must be easy to recover its SOC. Regarding the stability performance requirements vs the cost-effective battery charge, this is particularly difficult.

2.5 Charge/Discharge Cycle and Battery Lifetime

Battery cycle life is the total number of full discharges followed by full recharges. charging the device from 0% to 100% and then releasing the charge to return it to 0%. You are on borrowed time if your battery is older than that When a battery reaches its full cycle life, it doesn't immediately stop working. It begins to deteriorate more quickly, and it loses some of its full rechargeable capacity. Typically, battery life is computed using the battery's capacity in milliampere hours and the current rating in milliampere (mA) (mAh). The input current rating of the battery and the load current of the circuit may be used to determine the battery life. When the load current is low, the battery life will be high, and vice versa.

In particular, battery-powered renewable energy systems have evolved to rely heavily on energy storage. However, certain of the parameters during the charging and discharging operations are not under the user's control. The batteries age and have a shorter life span as a result of this unchecked use. It therefore results in an early replacement. Constant-current, constant-voltage controls are most frequently employed in the development of control systems because they aim to safeguard batteries and increase their lifespan. However, several studies demonstrate that model predictive control or fuzzy logic control can minimize charging time. Temperature control is an additional advantage. The assessment of current charging and discharging process control techniques in this research focuses on how they affect battery life. In order to determine the optimal way for real systems, both traditional and contemporary approaches are explored simultaneously [16].

Battery lifespan is influenced by a number of variables, including cell temperature, SOC, and others. The charge/discharge cycle of the battery, or DOD, has a substantial impact on battery life [26]. The expression for DOD can be as in equation (3) [27] :

$$\mathrm{DOD(k)} = \mathrm{DOD(k0)} + \frac{Ib\Delta k}{Cb} * 100\% \qquad \text{Equation (3)}$$

Where, Δk indicates change in period. The longer battery lifespan is negatively impacted by the larger charge/discharge current since it increases the chance of DOD. Using equation (4) lifetime of a battery (L_b) can be calculated.

$$Lb = \frac{1}{\sum_{m=1}^{N}\left(\frac{NCm}{CFdn}\right)} \qquad \text{Equation (4)}$$

where, NCm and CFdn represent the DOD's cycle count and cycle to failure, respectively. The value of m, which varies from 1 to N, determines the DOD period.

Online & quick-reacting Conventional units often provide PFR by raising or lowering their production in response to the detection of under- or over-frequencies (i.e., frequency 49.98 or frequency > 50.02), respectively. Grid-connected Li-ion BESSs function simply charging & discharging through the grid to offer downward and upward control. A restricted range of twenty milli hertz around the set point frequency is permitted. Typically, the PFR service must be provided linearly, according to the droop at frequency variations between twnty & two hundreds milli hertz from the set point frequency of fifty Hertz. Maximum power must only be provided for 15 minutes at a time, following which a 15-minute pause is permitted for the reserve to be re-established [28].

In our cases, if cycles per day is taken 0.5; SOCmax=1.0; SOC_{min}=0.2 and charging/discharging current as cases the battery life will be 12-15 years.

2.6 Sizing of BESS

Here, a strategy for scaling the BESS in terms of needed power and energy is described. Relating the terms inertial constant & droop, it depicts the BESS's contribution to the grid. The inertia constant and the power/frequency characteristic are used in this work to suggest an BESS sizing approach. The frequency response services (IR and PFR) that are the focus of this paper's target services demonstration. They are perceived as being "high power oriented," quick to react, and useful for brief periods of time (up to 15 minutes) [7].

$$H = \frac{Ekinetic}{Srated} = \frac{Jw2}{2Srated} \quad \text{Equation (5)}$$

$$-\frac{2Hsys}{f0} = \frac{\Delta Pb}{Ssys} \quad \text{Equation (6)}$$

$$R_i = \frac{-\Delta f/f0}{\Delta Pi/Si} \quad \text{Equation (7)}$$

$$H_{sys} = \frac{\sum_{i=1}^{n} Hi.Si}{Ssys} \quad \text{Equation (8)}$$

$$P_{bess} = S_{bess}\,(p_{ir} + p_{pfr}) \quad \text{Equation (9)}$$

$$Peff = \{Pbess/n_d \text{ for } Pbess>0;\ Pbess * n_c \text{ for } Pbess<0\ \}$$

$$\mathbf{SOC} = SOCinitial - \frac{\int Peff.dt}{Ebess} * 100 \quad \text{Equation (10)}$$

$$Sbess = Sps1 * \frac{Htarget - Hps1}{Hbess - Htarget} \quad \text{Equation (11)}$$

$$R_{total} = 1/\Lambda = \frac{f0}{\sum_{i=1}^{n} Si/Ri} = \frac{-\Delta fss}{\Delta P} \quad \text{Equation (12)}$$

$$S_{bess} = (R_{bess} * f_0).\ (\Lambda_{target} - \Lambda_{ps1}) \quad \text{Equation (13)}$$

$$Ebess = \frac{Treq.Sbess.\sqrt{nc}}{3600} + \frac{Treq.Sbess}{3600.\sqrt{nd}} \quad \text{Equation (14)}$$

The design requirements for the 50 Hz system under investigation were the highest magnitudes of the ROCOF(df/dt) of 0.5 Hz/s and the steady state frequency error fss 0.2

Hz in accordance with the grid code. The largest contingency event is thought to be the failure of generator G1 and the ensuing ΔP =150 MW power loss.

For our system considered,

H_1=9.55 s; H_2=3.33 s; H_3=2.35 s; t=900 s; n_c=n_d=0.85

Let's consider PV output of 150 MW and identical outage of conventional gen i.e. G3.

Base case (PS0):

Hsys = 5.82 sec; R_{total} =0.0044 or ʎ=227

Scenario first (PS1):

ʎ'=175; H'sys = 4.288 sec ;R'=0.00566

R_{bess} = 0.0036; H_{target} = 6.14; H_{bess} = 19.81 sec (from table @ Kir=1)

The IR with BESS using ……(viii)

$S_{bess} = Sps1 * \frac{Htarget-Hps1}{Hbess-Htarget} = 550 * \frac{6.14-4.288}{19.81-6.14} = 75.8 \approx 76$ MW

The PFR with ESS using ……(ix)

$ʎ_{target}$ =150/0.2 =750 MW/Hz

S_{bess} =(R_{bess}*f_0). ($ʎ_{target}$-$ʎ_{ps1}$) =0.0036*50*(750-175) =103.5 MW

Calculating the energy capacity of BESS for 15 min using ……(x)

$$Ebess = \frac{Treq.Sbess.\sqrt{nc}}{3600} + \frac{Treq.Sbess}{3600.\sqrt{nd}}$$

= 51.92 MWh

Hence analytical sizing of BESS is found to be nearly 105 MW and 52 MWh.

CHAPTER THREE. METHODOLOGY

3.1 Frequency Control with PV and NEM Grid Conditions

In order to ensure robust grid operation and prevent potential system outages, generating units must maintain the frequency range specified by the grid at all times. The unique nation grid codes, the kinds of fault events, and the length of the faults all have an impact on the frequency operating boundaries. The frequency operating criteria in this study are based on Australian NEM [29] . The non-critical frequency barrier is between 0.997 and 1.003 pu, whereas the limits for load/generation events and network events lasting five seconds are between 0.9 and 1.1 pu. The voltage's inoperative range is between 0.9 and 1.1 pu, and generating units' frequencies must under no circumstances deviate from those ranges. The main goals of adding the BESS are to fulfill grid functioning in accordance with the aforementioned criteria and offer extra oscillation dampening.

For the system to be able to support the grid with damping after any unforeseen disaster, it needs to have a sufficient energy reserve. The available output of generator or any other types of energy storages can be used to organize the energy reserve.

Within the NOFB, the steady-state frequency ought to be preserved. To preserve the standard frequencies or correct any under- or over-frequency actions, the generating unit should provide any transitory mismatches between the load demand and the generation. As a result, the governor's response to frequency changes with n generation systems can be expressed as in (15):

$$\frac{df}{dt} = \frac{fref}{2*\sum Hn}\Delta Pd \qquad \text{Equation (15)}$$

Whether fossil fuel power facilities are permanently linked to the current network or removed from it, the inertia of the system will decrease as the penetration of PV grows. Additionally, the grid could be unable to balance off any power imbalances because to the lower inertia and fluctuating PV output/network operating circumstances. In order to offer

frequency control and reduce the negative effects of PV, a BESS can be used, as shown in equation (6).

$$\frac{df}{dt} = \frac{fref}{Hb+2\sum Hn}\Delta Pd \qquad \text{Equation (16)}$$

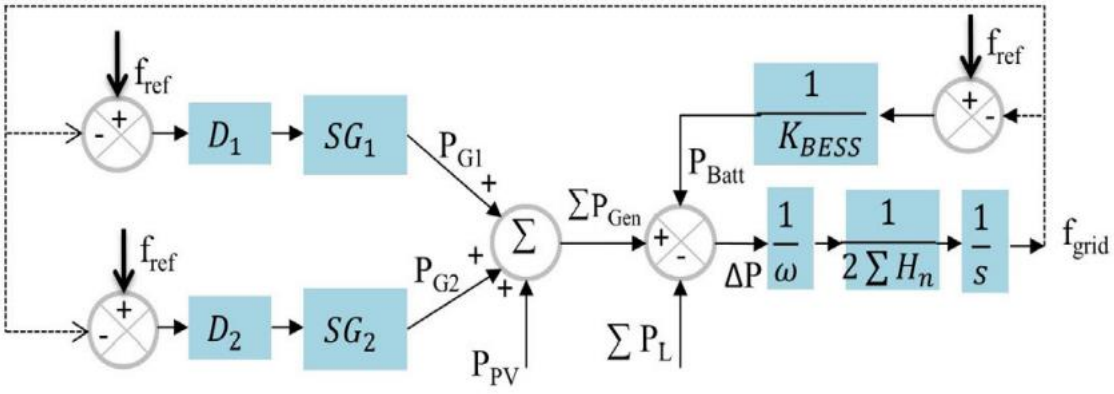

Figure 3.1: Frequency regulation of PV integrated system using BESS [30]

3.2 Voltage and frequency control using the overall BESS modeling

Figure 3.3 shows the basic layout of the BESS, which comprises of a battery bank, a power-conversing unit & if necessary, a transformer for HV-grid connectivity. Given that the battery SOC requirements are met, BESS controls its real & virtual power output on the basis of produced standard signals by the voltage and frequency controller. BESS's essential elements are as follows:

- Frequency controller;
- voltage controller;
- d & q -axis current controller;
- Real/Virtual (PQ) controller;

- Charge controller;
- Battery model.

The design of BESS in Dig SILENT/Power Factory is shown in Figure 3.2. The next subsection will provide a thorough overview of each controller.

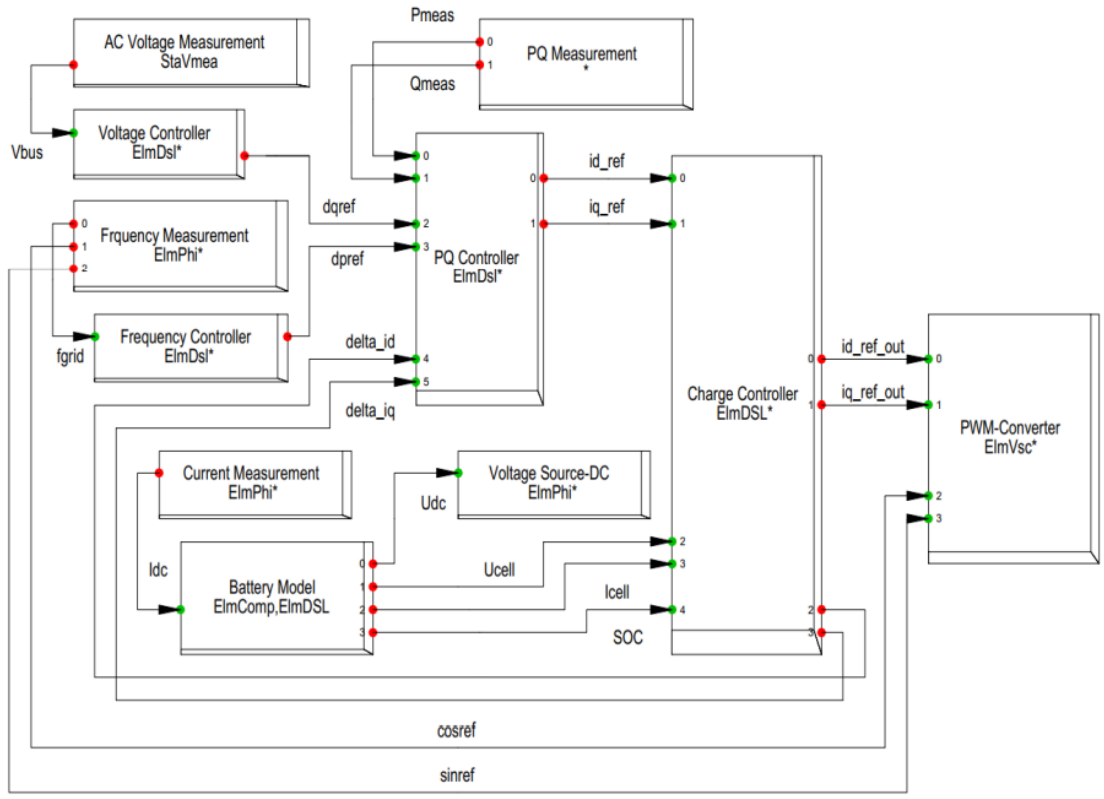

Figure 3.2: The model of BESS in Dig SILENT/Power Factory

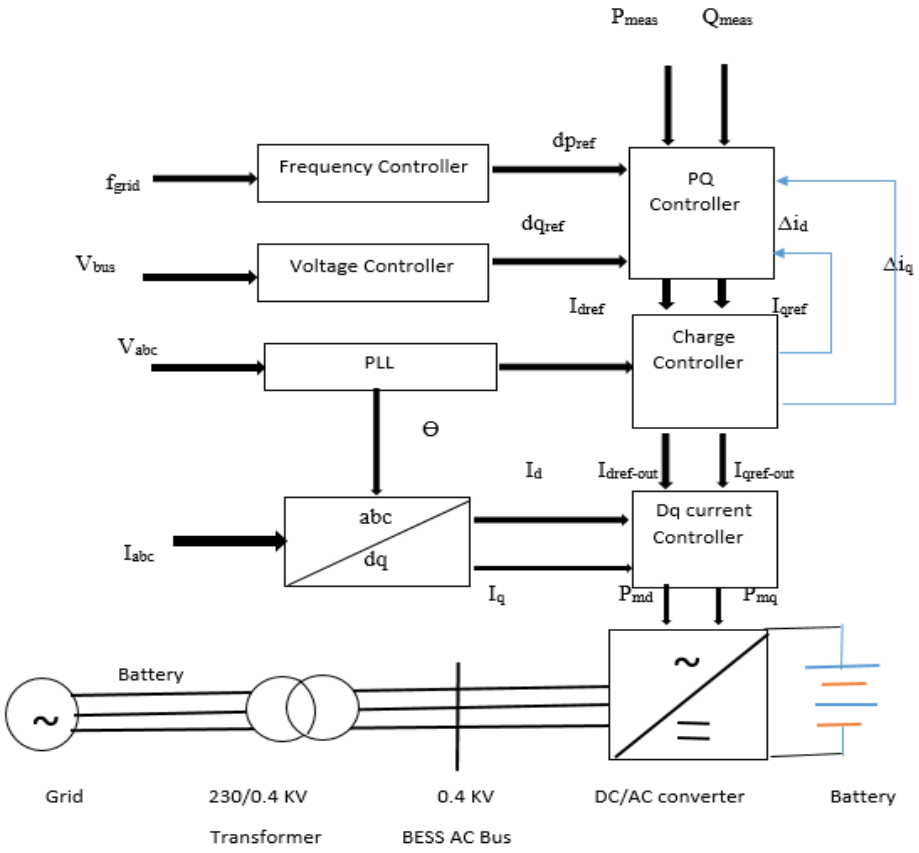

Figure 3.3: Primary frequency control with BESS [5]

3.2.1 Frequency Controller

Active power signal is produced by the difference between grid frequency and reference frequency. Then, to control BESS response, BESS power fluctuates in accordance with the frequency droop characteristics [4], as shown in Figure 3.4, and may be expressed as in (17).

$$\mathbf{\Delta P} = \frac{1}{\text{Rbess}} (f_{ref} - f_{grid}) \qquad \text{equation (17)}$$

Where $1/R_{bess}$ is the slope of frequency droop and fref is the frequency reference (1pu). If Δf is positive, the BESS drains active power; if Δf is negative, the battery is charged.

According to NEM, the dead band, which designates the deactivation limit, is 0.003 pu of the standard frequency. According to BESS droop characteristics, Real power control in Figure 3.4 creates an active current signal.

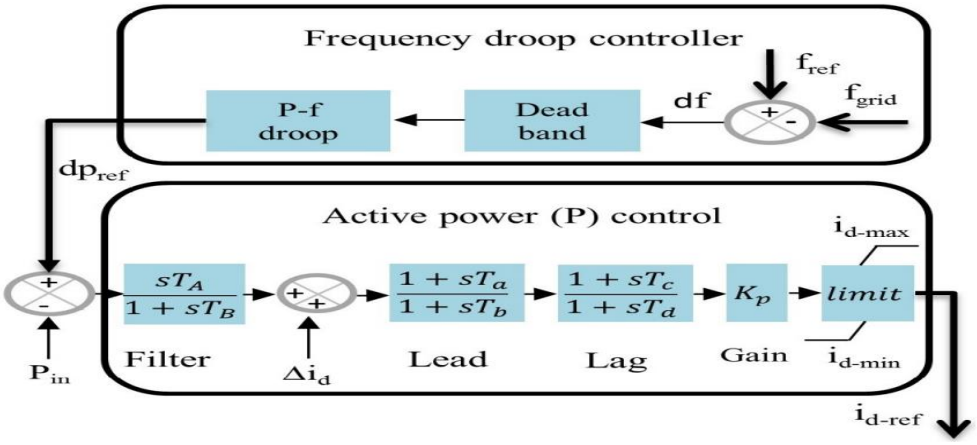

Figure 3.4: Frequency and active power control of BESS [31]

Through the PLL, this controller receives the measured frequency signal from the grid. The droop and deadband settings for the frequency controller are both set to 0.004 [pu] and 0.003 [pu], respectively. In this instance, the specified droop indicates that the full active power will be engaged when the frequency deviation is higher than or equal to 0.2 [Hz], whilst the deadband shows that there will be no control activation for the frequency magnitude within the range of [49.85 50.15] [Hz].

When considering deviations in frequency from the reference value as described in equation (18), the droop establishes the ceiling for triggering the maximum active power.

$$dPref = \frac{\pm \mathrm{df}}{droop(Rpf)} \qquad \text{Equation (18)}$$

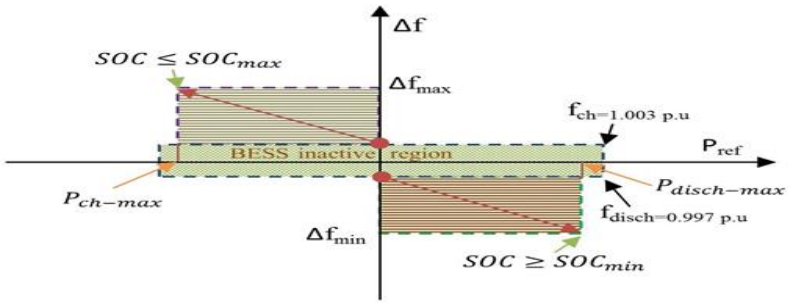

Figure 3.5: p-f droop chac [3]

3.2.2 Voltage Controller:

In order to manage the BESS reaction as in Fig.3.6, the voltage controller generates the virtual power signal on the basis of mismatches between the real & standard bus voltage as in equation (19).

$$\Delta Q = \frac{1}{Rbess}(v_{ref} - v_{bus}) \qquad \text{equation (19)}$$

Where $1/_{Rbess}$ is the voltage droop's slope and V_{ref} is the reference (pu).

The +ve (supply) or -ve (consume) sign of Δv determines whether the BESS contributes reactive power. 0.04 pu of the standard voltage magnitude is chosen as dead band value for voltage control. The battery capacity that remains after supplying active power is the quantity of reactive power.

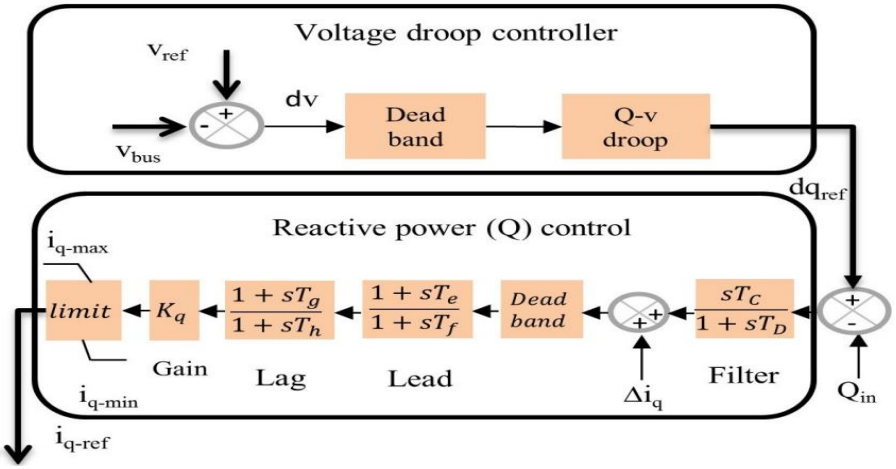

Figure 3.6: Voltage and reactive power control of BESS [5]

The droop establishes the maximum voltage at which the whole reactive power can be activated in response to deviations from the reference value as specified in equation (10):

$$dQref = \frac{\pm \mathrm{dv}}{droop(Rqv)} \qquad \text{Equation(10)}$$

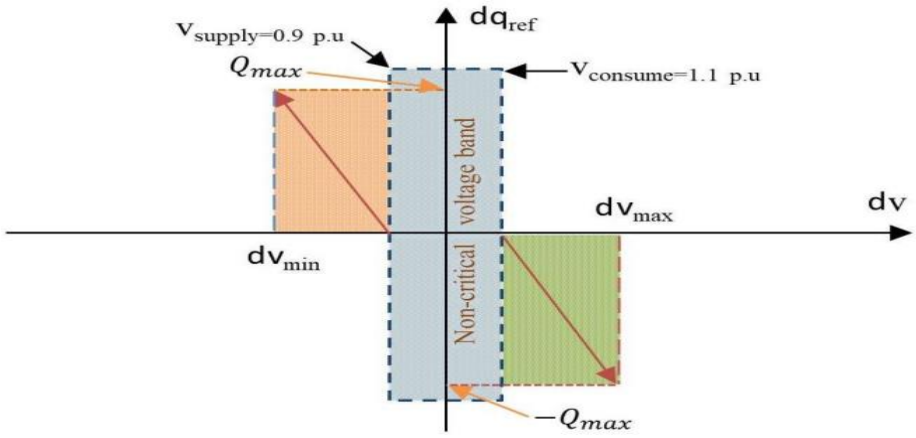

Figure 3.7:Voltage droop characteristics [5]

3.2.3 Active/Reactive power(PQ)controller:

"Based on the active power error between P_{ref} and P_{in} and Δi_d from the charge controller, the first order filter, and a proportional-integral (PI) controller, the active power (P)

provides an active power reference signal. When considering the reactive power error between Q_{ref} and Q_{in} as well as Δi_q from the charge controller, the first order filter, and the PI controller, the reactive power (Q) provides the reactive power reference signal." Figure 3.8 shows the charge controller, d and q axis controller.

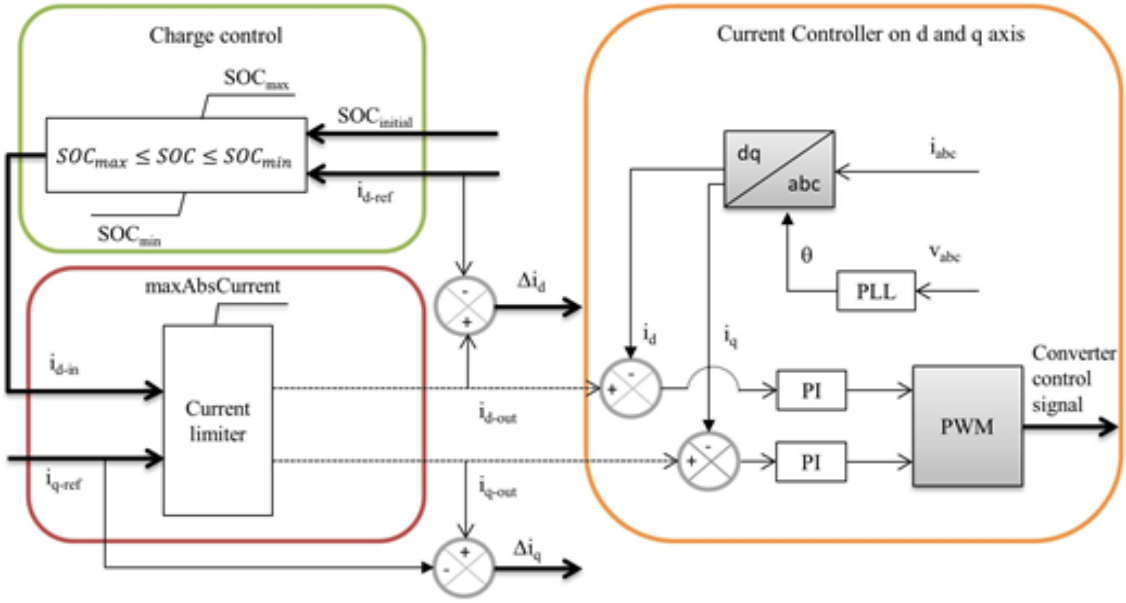

Figure 3.8: Charge controller ,d & q-axis controller [3]

3.2.4 BESS charge control and Charging management

BESS reduces oscillations to lessen short-term power imbalances by absorbing excess energy or supplying a lack thereof. The NOFB border fluctuates around df=150 mHz. The maximum BESS capacity in a 50Hz system is triggered for a frequency change of 0.2 Hertz according to the droop gain of 5. As shown in, the P-f droop retains a linear relationship (7). If the SOC of battery meets the requirements as shown in Figure 3.8, battery current flows in the opposite direction of frequency variations. A flexible BESS operation that may be adjusted to the needs of the BESS operator is made possible by an efficient charge/discharge management technique.

State-of-charge (SOC) techniques are described in this paper and are used to regulate battery charging or discharging.

3.2.4.1 Droop-type battery charging/discharging method

The fundamental droop-type battery charging/discharging method is expressed as follows:

$$I_{d\text{-}in} = \{i_{d\text{-}ref} \text{ if } SOC \geq SOC_{min};$$

$$-i_{d\text{-}ref} \text{ if } SOC \leq SOC_{max};$$

$$0 \text{ if } SOC_{max} < SOC < SOC_{min}\}$$

If the battery SOC is greater than 0.2 per unit (the lowest soc), BESS can provide real power; if it is lesser than 1 pu, it can absorb active power (maximum SOC). The highest possible magnitude of 1 per unit, which denotes the overall size of the BESS controller, places restrictions on the real & virtual power references on the d-axis & q-axis respectively. The active and reactive power error is calculated in the PQ controller by adding the difference between the input and output of the charge controller's d axis current as Δi_d and q axis current as Δi_q.

Battery charging and discharging causes a change in battery SOC, which will either rise or fall depending on how much active power is exchanged during transient times. Additionally, battery self-discharge will lower the soc of battery. As a result, less battery capacity is available to react to upcoming events. An efficient recharging approach must be devised to prevent reduced SOC or significantly oversizing the BESS capacity, which might potentially increase system reliability and lower associated costs:

3.2.4.2 Technique Recovering SOC

To provide sufficient BESS capacity for upcoming contingency events, the battery should be recharged since the battery SOC fluctuates when energy is transferred during frequency regulation. Instead, it's important to ensure that SOC levels are kept low enough for BESS

to participate in over-frequency events. As a result, the SOC charging ceiling must not exceed the maximum SOC. As a result, battery charging recovery may be expressed as:

$$I_{d\text{-}in} = \{i_{ch\text{-}cur} \text{ if } SOC \leq 0.5 \text{ or } SOC \leq SOC_{min}$$

$$\& \; i_{d\text{-}ref} < 0.0001$$

$$0 \text{ if } SOC < SOC_{max}\}$$

If the battery's SOC and active power current reference are less than 0.5 pu and 0.0001 pu, respectively, the battery should be recharged until the SOC meets the upper limit. The regulation that lowers the battery recharge threshold below the maximum SOC promotes the use of a designated frequency reserve to address over-frequency concerns.

$$SOC_{max} = \{SOC_{adaptive} \text{ if } i_{ch\text{-}A} > i_{ch\text{-}threshold}$$

$$SOC_{max} \text{ if } i_{ch\text{-}A} \leq i_{ch\text{-}threshold}\}$$

As per aforementioned criteria, SOCmax is the SOCadaptive) for a charging current more than the benchmark & SOC_{max} for a charging current less / equal to benchmark level. The charge benchmark level of 0.1pu is chosen to be used. As a result, 1pu is the maximum SOC value for a charging current of 0 to 0.1pu. The adapted SOC value will be chosen if the charging current is more than 0.1pu & the maxSOC limit for adapted SOC is set to be 0.8pu. The charging threshold and maximum adaptive SOC limit are constantly subject to change in line with the BESS operator's strategy, so keep that in mind.

3.2.5 Dq current controller

By regulating d and q axis current using a PI- control, this controller controls BESS active and reactive power. The converter's alternating current in d-q frame of reference works as the feedback signal. The DC/AC converter operation is controlled by a pulse with modulated signal, which is the resulting signal of d-q controller. The observed dq axes values at the output of the BESS converter and the d-q references output $i_{d\text{-}ref\text{-}out}$ and $i_{q\text{-}ref\text{-}out}$ are the inputs for the current controller. To supply the referenced phase angle needed to drive the converter, the PLL converts the PWM index in the d and q axes (p_{md} and p_{mq}, respectively).

3.2.6 Sample Battery

An analogous electrical network description of a battery is taken into consideration because it is still difficult to accurately simulate chemical reaction-based batteries. This work's battery model, which treats the battery as a DC source with an internal resistance, is accessible in [32].The battery is a component of the BESS that stores charged energy in the form of chemical energy, which is later released as needed in the form of electric power. The battery model that was designed has a rating of 40 [kWh] of energy and 5 [kW] of power. It should be noted that since the Vanadium Redox Flow battery model is currently unavailable in PowerFactory, the battery in this project is being modeled as the voltage source. Equations (11), (12), and (13) are used to dimension the battery, and Table 3.1 contains the requirements that were employed.

$$V_{cell} = V_{max} \cdot SOC_0 + V_{min} \cdot (1 - SOC_0) \qquad \text{equation (11)}$$

$$V_{term} = V_{cell} \cdot n_{row} /1000 \qquad \text{equation (12)}$$

$$E_{batt,rate} = C_{cell} \cdot n_{parallel} \cdot V_{term} \qquad \text{equation (13)}$$

Table 3.1: Battery settings

Parameter	Value
SOC_0 (Initialization) [pu]	0.8
Capacity of each cell [Ah]	80.
V_{min} [V]	12.
V_{max} [V]	13.85
Parallel cells	60.
Cells in series	65.
V_{nom} Nominal voltage of source [kV]	0.9
R_i Intern resistance per cell [Ω]	0.001

3.2.7 Photo-voltaic (PV)

The Dig SILENT Power Factory standard model for PV systems was used in this research. The specified irradiance data and timing are the primary determinants of the generated power. Equations 14 and 15 are used to determine this [33].

$$P_{panel} = \frac{Eg,pv * Ppk,panel * \eta rel * \eta inv}{Estd} \qquad \text{Equation(14)}$$

$$P_{system} = P_{panel} * Num_{panels} \qquad \text{Equation (15)}$$

Where:

• Ppanel: Active power output of the panel in [kW]

• Psystem: Single system active power output in [kW]

• Num_{panels}: Number of panels per inverter

• Eg, pv: Global irradiance on the plane of the array in W/m2

• EST D: Standard irradiance value of 1000W/m2

• Ppk, panel: Total rated peak power of the solar panel in [kW]

• ηrel: Relative efficiency of the panel • ηinv: Efficiency factor of the inverter

The further description of the PV model can be seen in Appendix A.

3.3 ATTRIBUTE OF THE TEST SYSTEM AND CASE STUDIES

3.3.1 Attribute of the test system

Modified IEEE 9 bus system

On a modified IEEE 9 bus system, as illustrated in Figure 3.9, the amount of PV penetration and its effects are evaluated [3]. The Dig SILENT power factory is where the RMS/EMT simulations are run. The three synchronous generators G1, G2, and G3 are each simulated as a hydroelectric plant, a gas turbine, and a coal plant, respectively, with a turbine, governor, and AVR. [2] contains information about network modeling in depth. BESS is put at bus 7 since it is the best site, while PV systems are installed @ bus-9 using a 0.4/230 kilo-volt trans-former. [33] contains the detailed modeling of the PV system. This study's goal is to replace third generator units & provide additional solar to the network. Using a both directional dc to ac converting device & one 0.4/230 kilo-Volt trans-former, the BESS is linked to bus 7.

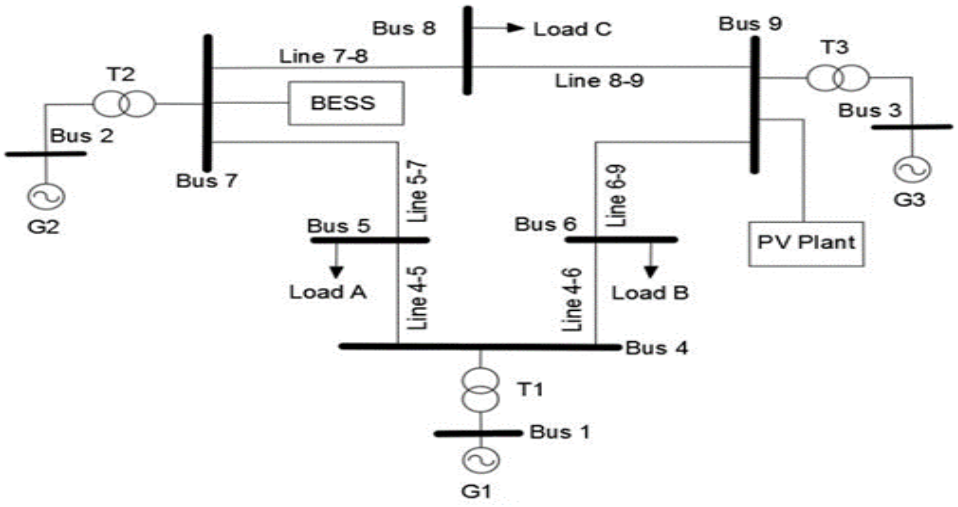

Figure 3.9: The WSCC system with PV & BESS location [36]

Modified IEEE 14 bus system

Three of the five synchronous machines with IEEE type-1 exciters that make up the modified IEEE 14-bus test system are synchronous compensators that are exclusively utilized to supply reactive power. There are 11 constant impedance loads, 19 buses, 17 transmission lines, and 8 transformers. 259 MW and 73.5 MVAr are required for the entire load [34]. Figure 3.10 illustrates the single line diagram. It is a streamlined representation of the Midwest United States transmission system. BESS is put at bus 6 as it is the best site, while PV systems are installed at bus 8 using a 0.4/220kV transformer. [33] contains the detailed modeling of the PV system. At bus 6, a 0.4/132 kV transformer connects the BESS to the grid.

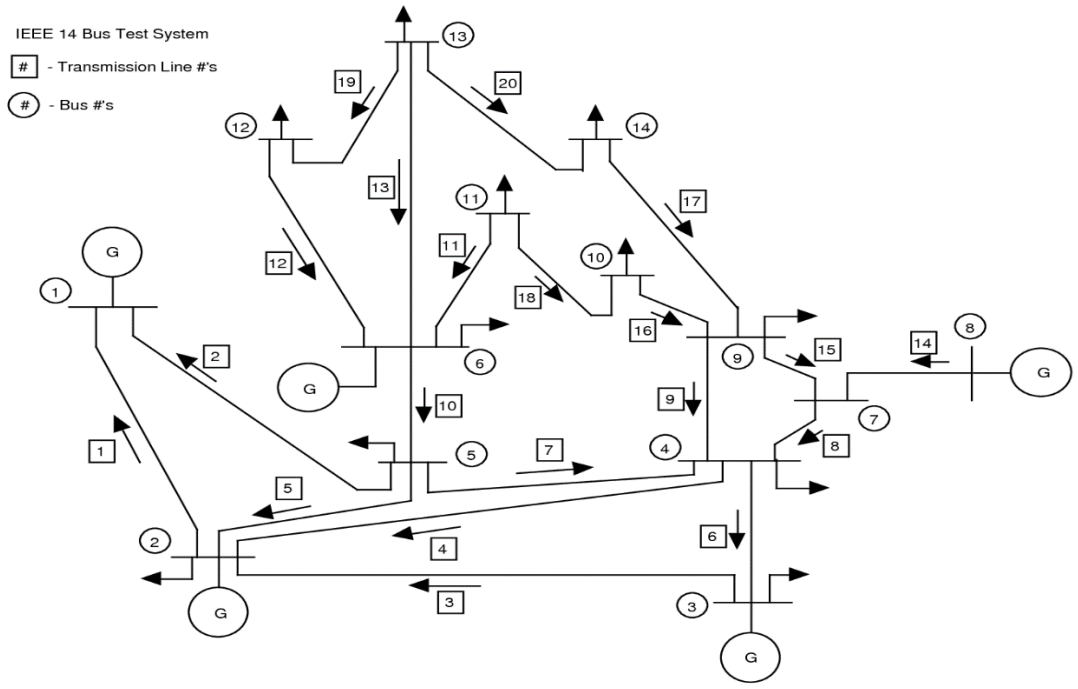

Figure 3.10 : Modified IEEE 14 bus system network [34]

The representation of PV penetration is calculated as in (13):

$$\%PV_{penetration} = \sum P_{pv} / (\sum P_{pv} + \sum P_{sg}) \quad (13)$$

where, $\sum P_{pv}$ and $\sum P_{sg}$ represent the combined MW output power of the PV and SGs units. The degree of PV penetration and how it affects total system inertia depend on two key factors, which are as follows:

- In spite of the degree of PV addition, existing conventional unit continue to run.
- PV integration displaces existing SG units.

3.3.2 Low and Heavy Load scenarios

The simulations are carried out for various PV penetration levels with varying contingencies and loads as shown in tables I and II. Two distinct generation techniques are described in Table II for low load conditions.

Table 3.2: Load profile (MW) in Different Operation Modes

	L_A	L_B	L_C
Low Load	100	90	90
Heavy Load	170	110	110

Table 3.3: Gen output at different operating strategy

Strategy	Gen1/MW	Gen2/MW	PV/MW
Strategy- I	90 (29%)	80 (32%)	150
Strategy- II	140 (48%)	60 (25%)	150

3.3.3 Scenarios Considered

Following two distinct scenarios are performed which depicts the level of PV penetration and its effect on power system rely on PV installation point and fault type.

- scenario 1: Low load and generator control during a line event
- scenario 2: Heavy load and both temporary and permanent line outages

While strategy 2 refers to irregular loading conditions for generators, strategy 1 stipulates 150MW PV penetration with typical operation of conventional generators. At light load, the active power consumption is 280 MW, while at heavy load, it is 390 MW.

CHAPTER FOUR. RESULT AND DISCUSSION

"Two contingency events, a line outage and a load event, are undertaken to examine the inertial impact of PV penetration and the efficacy of various operational strategies utilized by SGs in maintaining grid standards both with and without a BESS." Additionally, while preserving grid-defined frequency standards, the installation and size of BESS are also investigated. Two IEEE systems are used to study the PV penetration, operation methods, and the suggested BESS charging mechanism i.e. modified IEEE 9-bus system & modified IEEE 14 bus system as shown in Figure 4.1 & Figure 4.12 respectively. The PV farm is linked to the grid by an appropriate step-up transformer, and the PV output is taken into account as an aggregate output. With the penetration of PV, the fossil fuel generating unit is totally turned off. BESS integration aims to offer grid dampening, enhance transient performance, and meet grid standards. RMS/EMT simulations are done for all scenarios in Dig silent power factory environment.

4.1 Modified IEEE 9 Bus System

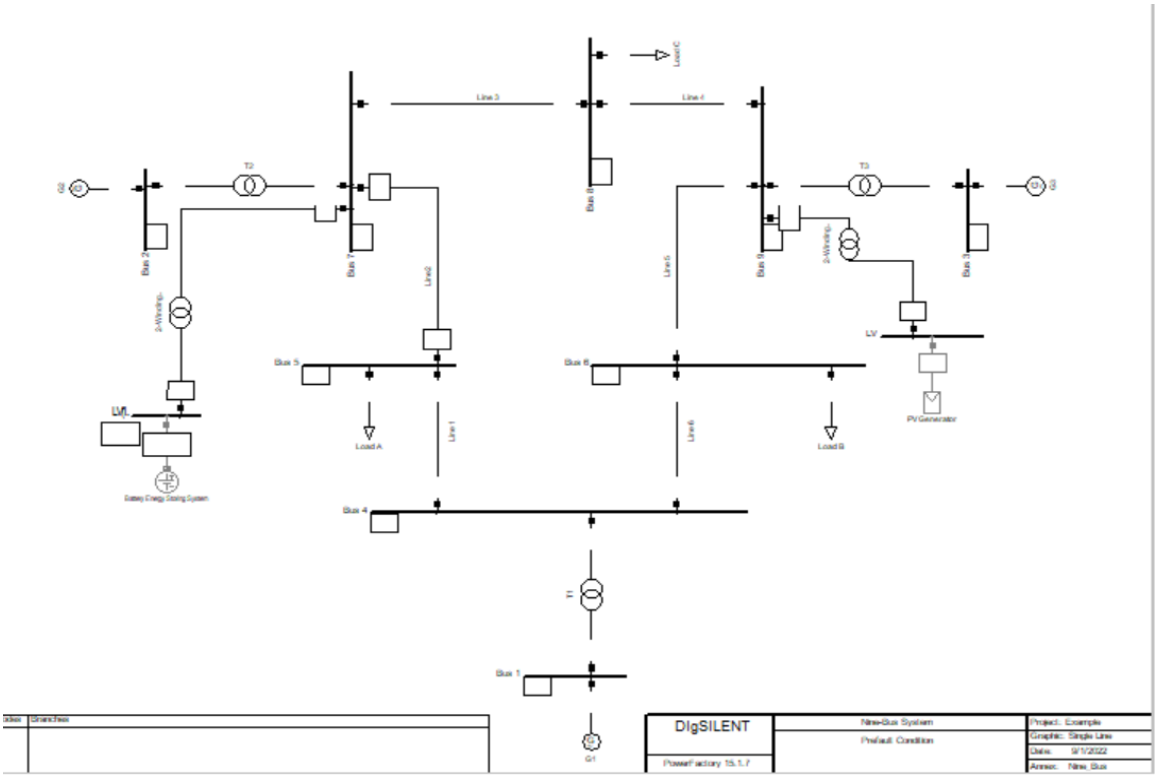

Figure 4.1: IEEE 9 bus system in Power Factory

4.1.1 Light load and generator control during a line event

One of the frequent network occurrences in the power system is a line outage, which is typically caused by downed trees or damaged power poles. “A temporary line outage of lines 5-7 and a permanent outage of lines 8–9 are included while analyzing the transient performance of the grid. A single-phase-to-ground fault is applied on lines 5-7 and 8-9 at t=0 s. The transient line fault on line 5-7 is resolved at t=0.24s.” The line is permanently eliminated at t = 0.24 s, removing the line 8–9 permanent fault. Low load and 100 MW of PV penetration are examined with two different generator operating strategies.

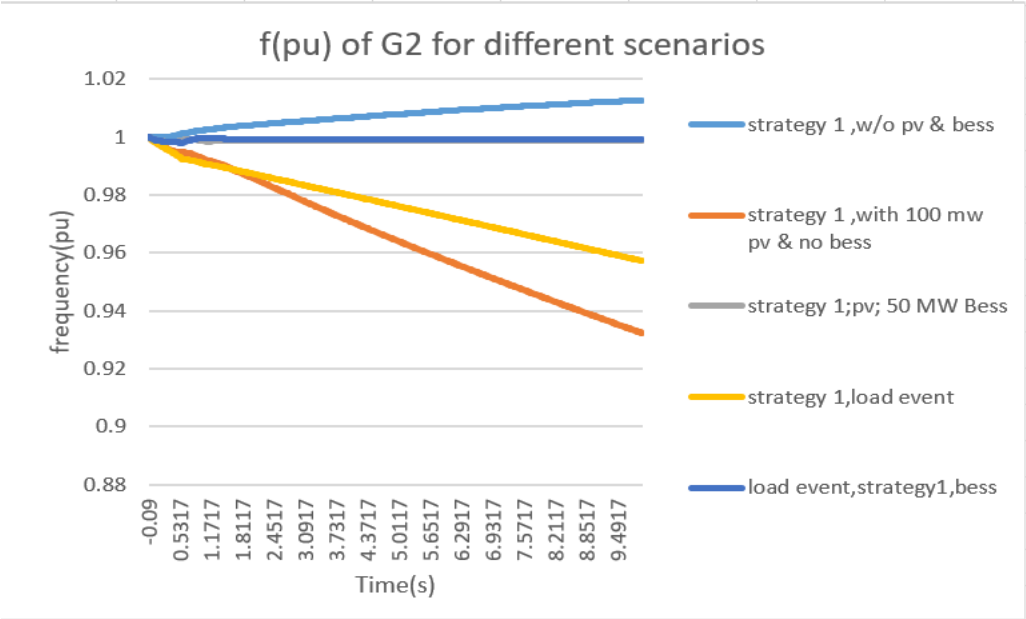

Figure 4.2: The frequency of G2 (pu) for various Scenarios

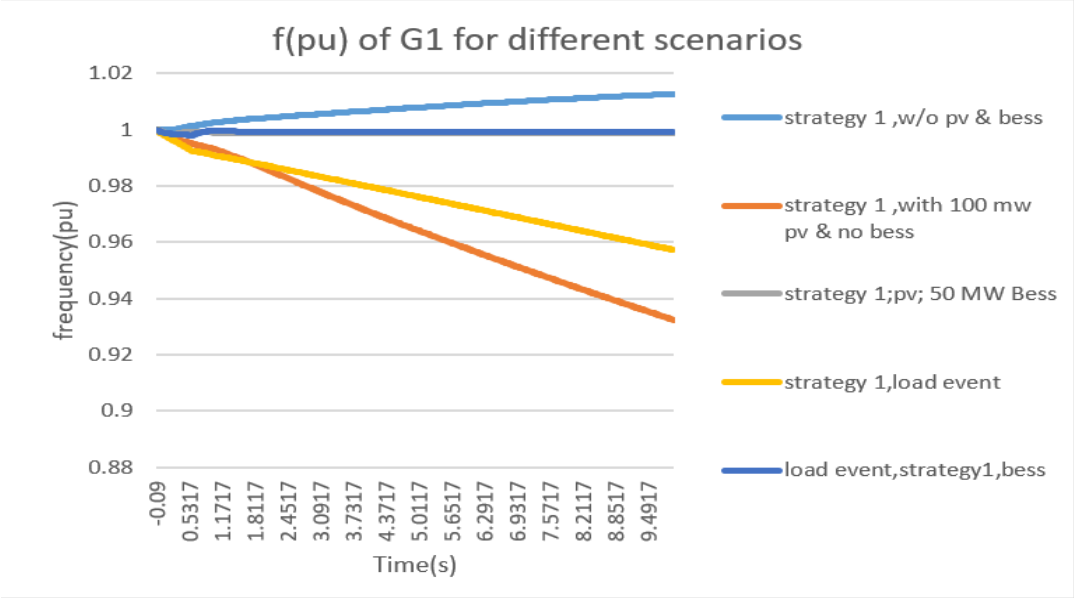

Figure 4.3: The frequency of G1 (pu) for various Scenarios

Figure 4.2 & 4.3 depict the grid's performance under various network operating conditions. When using strategies, I & II without PV addition it can be shown that the oscillating frequency of G2 remain below 2% of standard magnitude referred by the NEM-grid-code. The operation of Strategy I & 100MW of PV generation results in an increase in frequency deviation, although it stays under the grid limit. Generators have a greater margin of control when running at lower power output (operating strategy 1), which gives them the capacity to contribute to oscillation damping. But for G1 and G2, the frequency increases by 0.15Hz & 0.19 Hz respectively.

Table 4.1: Various scenario & network contingencies and their impact on frequency

Operation scenario	PV-No (Hertz)	PV-Yes (Hertz)	PV &BESS (Hertz)	Gen-set
Strategy-1 Strategy-2	50.45 50.70	50.60 51.02	 50.365	1
Strategy-1 Strategy-2	50.67 50.90	50.86 51.23	 50.487	2

4.1.2 Heavy load and both temporary and permanent line outages

The earlier mentioned faults are applied for heavy load case. The output is seen complying the grid code with scenarios with no PV generation and with PV generation of 60 MW i.e.1.0072 pu (50.36 Hz). However, with 100 MW and increased PV generation the system breaches the grid compatibility requirements by failing to offer damping support as shown in Figure 4.2. The generator G1 has a similar reaction to that in figure 4.3 above.

On the other hand, while using strategy 2 and generating the same amount of PV, variations in the frequency of G1 & G2 are extremely oscillating and exceed the required grid limit by 1.0204 (G1) and 1.0246pu (G2), respectively. The generators' power margin is decreased in "operation strategy 2," though, and as a result, they are unable to supply enough damping to uphold the grid's established operating criteria. Table 4.1 displays the increase in frequency deviation for operating strategy 2 and PV penetration. In order to maintain frequency variations within the necessary grid restrictions and provide additional oscillation damping, a 50 MW BESS (4.5 MWh) is integrated into the grid.

This data demonstrates that BESS is crucial for reducing the impact of PV penetration and meeting the grid restrictions. In addition, as demonstrated in Figure 4.4, BESS reduces generator oscillations in active power when compared to no BESS.

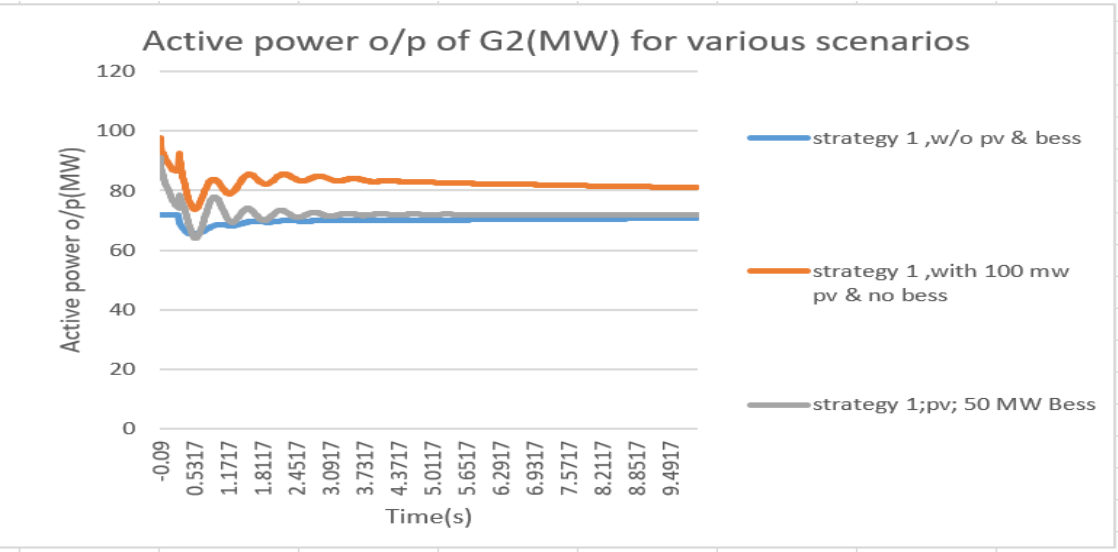

Figure 4.4: Active power output(MW) of G2

Figure 4.5 displays the voltages at bus 7/Bess connection point for various operation scenarios. As can be seen, the voltage loss is largest when PV penetration and operating strategy 1 are used in comparison to neither PV nor operating strategy 1. As reactive power is added to the system during a voltage drop and harmonics are reduced rapidly to other scenario, it can be shown that BESS greatly improves the voltage profile.

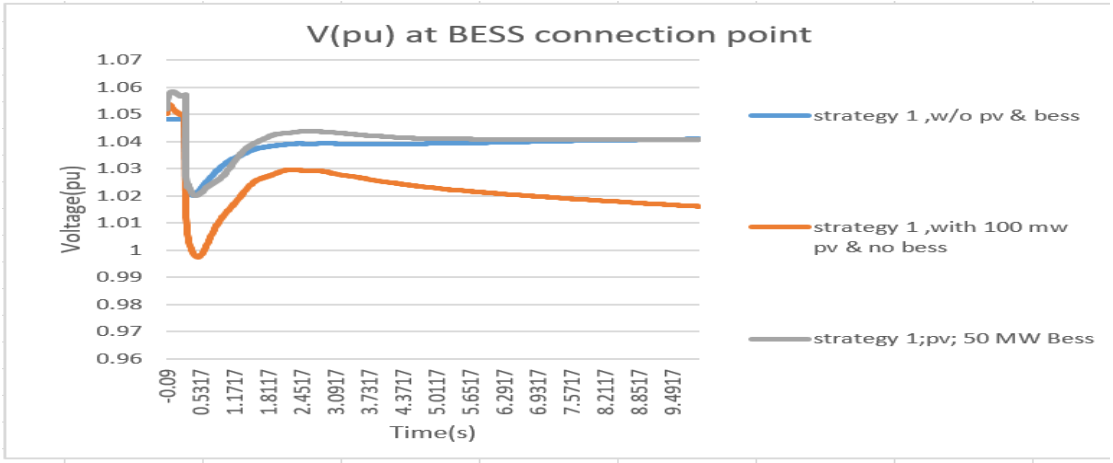

Figure 4.5: Voltage at BESS connection point

The voltage response of G1 & G2 for different scenarios are shown in Figure 4.6 & Figure 4.7 respectively. These findings demonstrate that, in the presence of disturbances, BESS enhances the voltage profile and speeds up system stabilization. Additionally, it has been shown that, in comparison to the absence of a BESS, the BESS significantly reduces the active power oscillations of the generator. The generator G1 exhibits a comparable degree of enhanced performance with BESS.

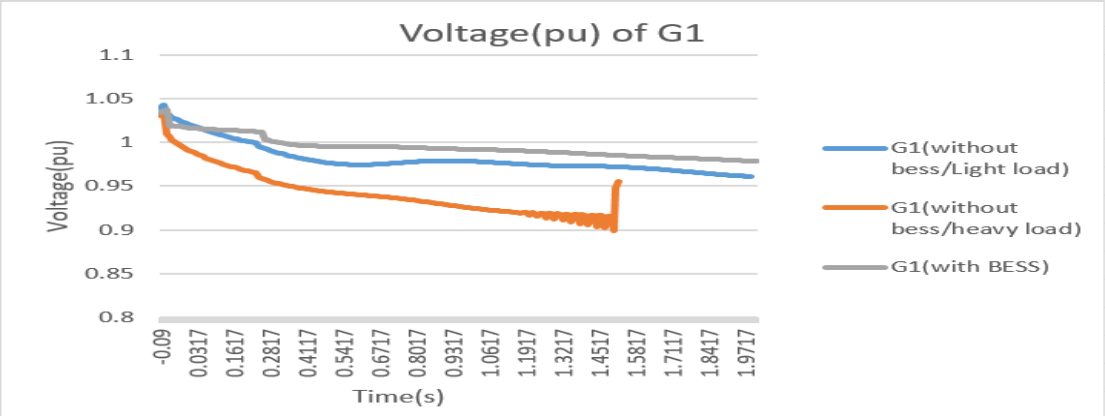

Figure 4.6: Voltage [pu] for different scenario

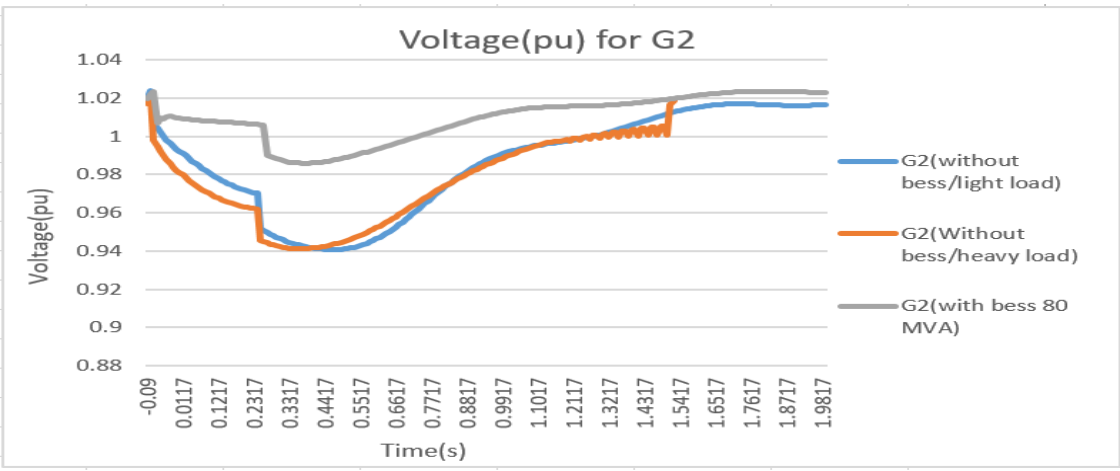

Figure 4.7: Voltage [pu] for different scenario

The BESS's real & virtual power transfer in transitory is presented in Figure 4.8. Because of narrower frequencies boundary control & higher precedence given to real power over virtual power, it can be observed that a significant quantity of active power as opposed to reactive power participates in frequency regulation.40 MW and 6 Mvar are the maximum exchanged value of active and reactive power of BESS respectively.

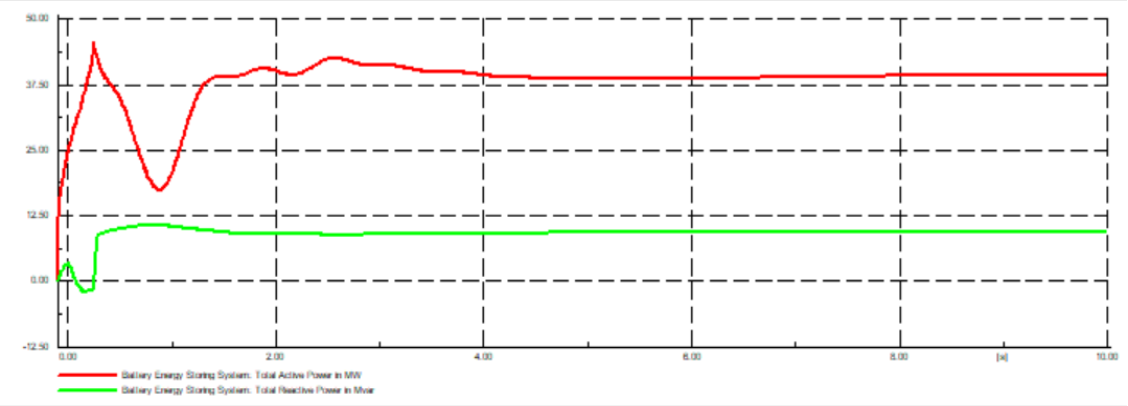

Figure 4.8: BESS active and reactive power

4.1.3 BESS installation location & sizing

To provide the desired outcome while using a BESS converter and energy capacity as minimal as feasible, the placement of BESS is crucial. This can help to lower losses and the total expenses of BESS. As a result, the integrated BESS is put at various buses throughout the network to examine its performance under the two contingency events under consideration. By deploying BESS at various buses, a comparative performance study of the location and converter size of the system is conducted. It has been discovered that all locations are not ideal for placing BESS because the grid cannot maintain frequency oscillations under criteria of the grid even with the rated BESS capacity. Even though SG1's frequency remains below the ceiling when BESS is deployed in the network, only the bus 7 satisfies the grid's requirements in the case of SG1. Thus, given the line outage and load event, it can be said that bus 7 is the best place for implementing BESS. The BESS is placed at three different locations and rotor angle vs. time is observed for generator 2 and it is found fast dampening of gen at bus 7 and hence it is concluded as optimal locations. Figure 4.9 shows that BESS secures network performance in accordance with grid compatibility and provides suitable dampening to the system frequency. Also frequency plotted for the cases is shown below Figure 19 & Figure 20.

Hence, a 50 MW of converter size is depicted from comparative performance analysis. Hence, BESS of size 50 MW is installed at bus 7 to provide required frequency support to the system.

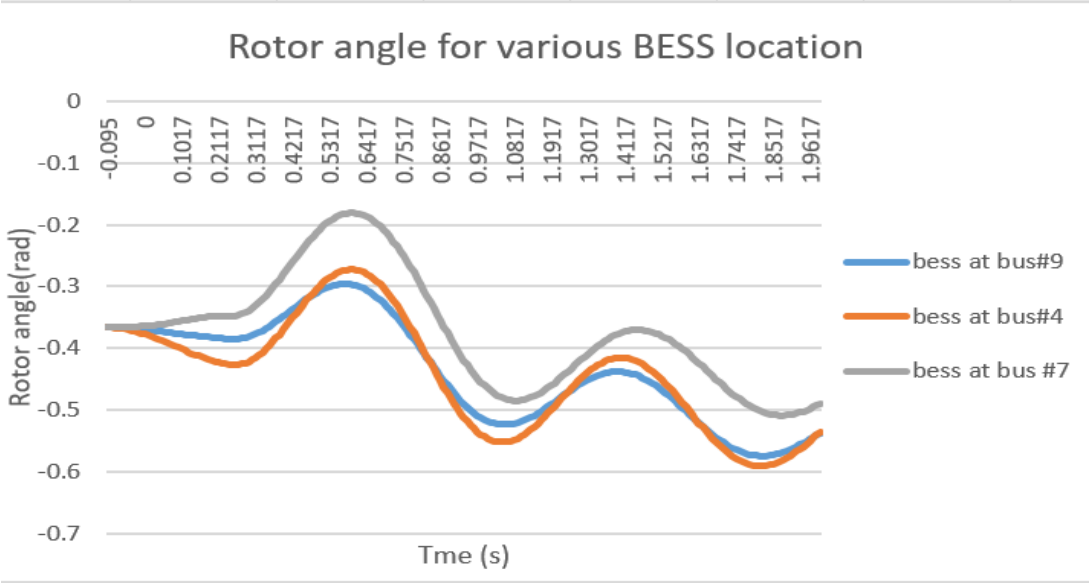

Figure 4.9: Rotor angle plot of G2 for various BESS location

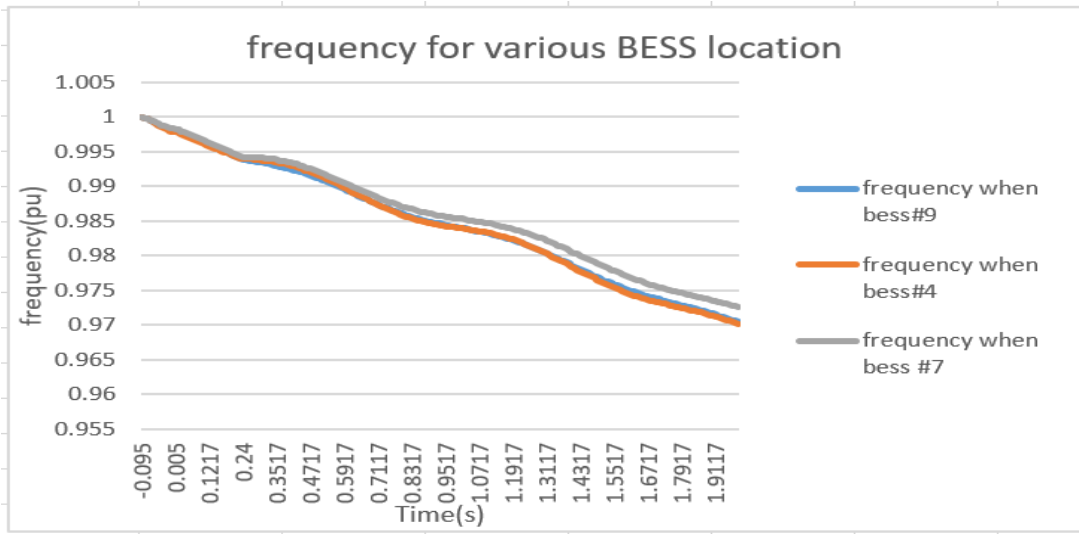

Figure 4.10: frequency plot of G2 for various BESS location

4.1.4 BESS Recharging

The self-discharging properties of the battery as well as the interchange of BESS power with the grid cause fluctuations in battery SOC. To guarantee that the cell is sufficiently charged to take part in power exchange anytime, a SOC recharge facility is necessary. The battery's state of charge variations during event intervals are displayed in Figure 4.11.

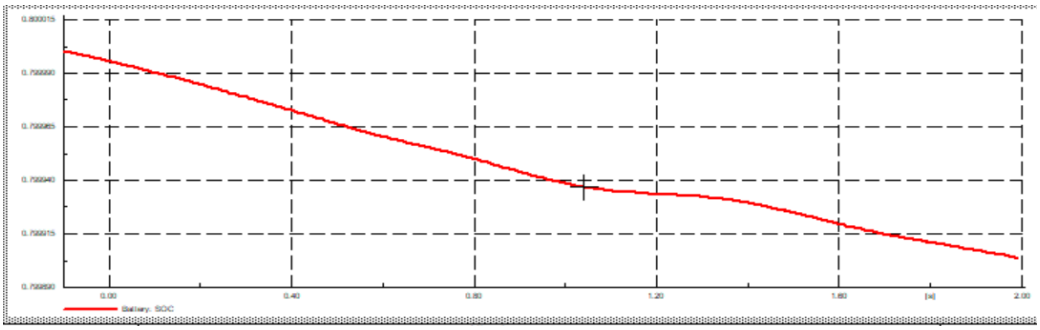

Figure 4.11: Battery recharging scenarios

4.2 Modified IEEE 14 Bus System

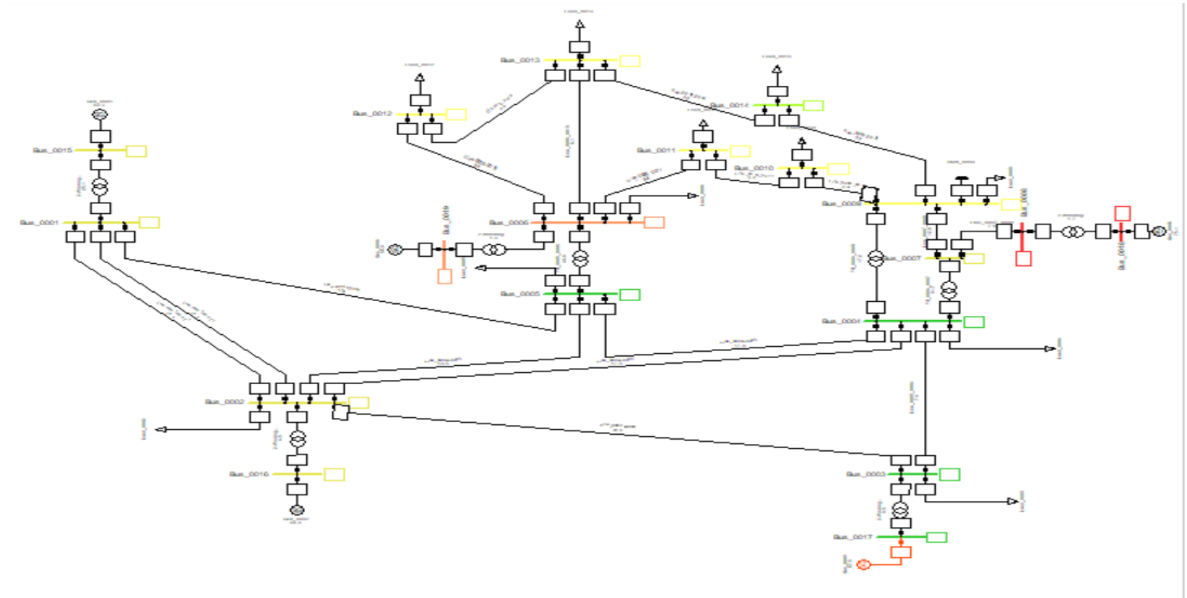

Figure 4.12: Modified IEEE 14 bus system

4.2.1 Light load and generator control during a line event

For the purpose of studying the transient performance of the grid, a short circuit event @ t=0.2 sec on line 6-12 and line 9-14 are taken into consideration. On lines 6-12 and 9-14, a L-G fault is injected at t=0.2 s. At t=0.4 the transient line fault On lines 6-12 and 9-14 are cleared. Low load and 140 MW of PV penetration are examined with two different generator operating strategies.

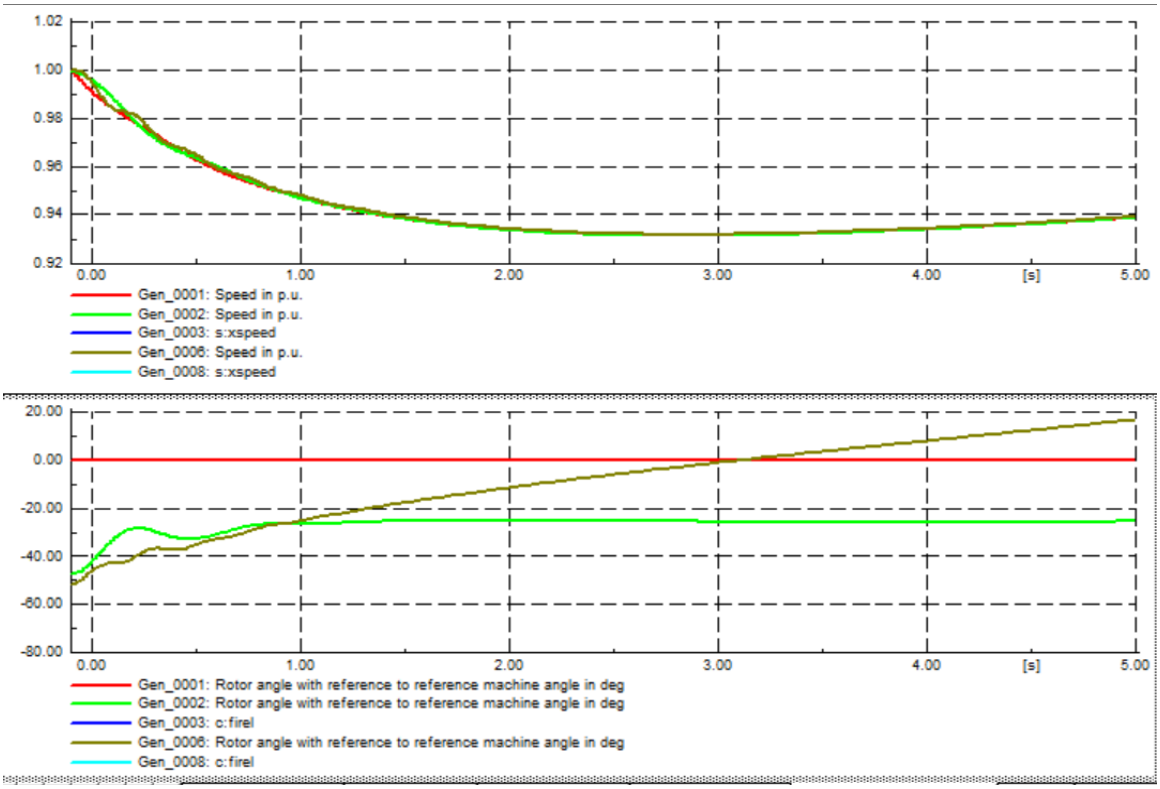

Figure 4.13: Scenario 1 plot for speed and rotor angle

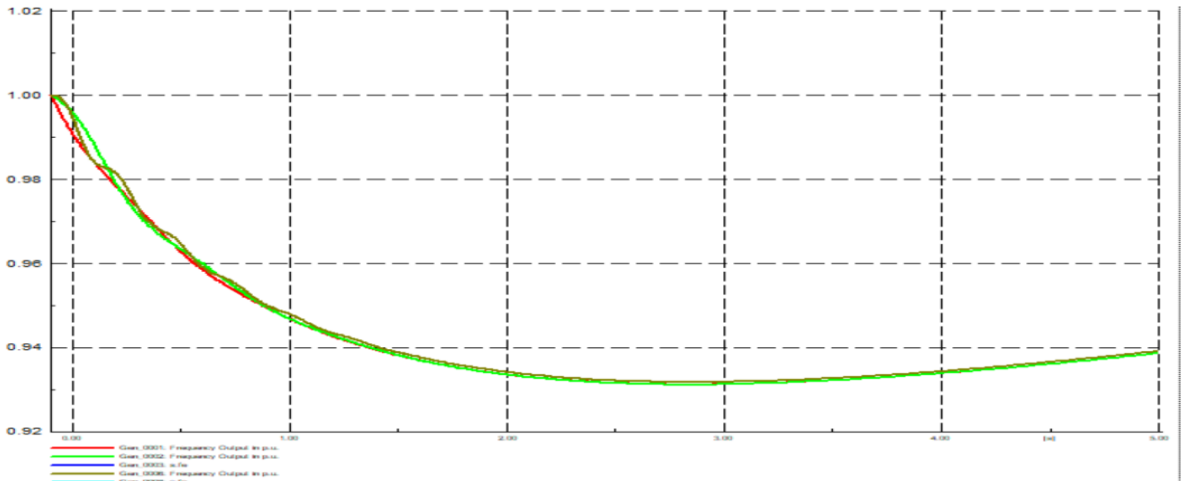

Figure 4.14: Scenario 1 Frequency plot for all gen

Figure 4.13 & 4.14 depict the grid's performance during line contingencies and pv penetration scenarios. As can be observed, G1 and G2's frequency oscillations exceeded the nominal value by 2% as prescribed by the NEM grid.

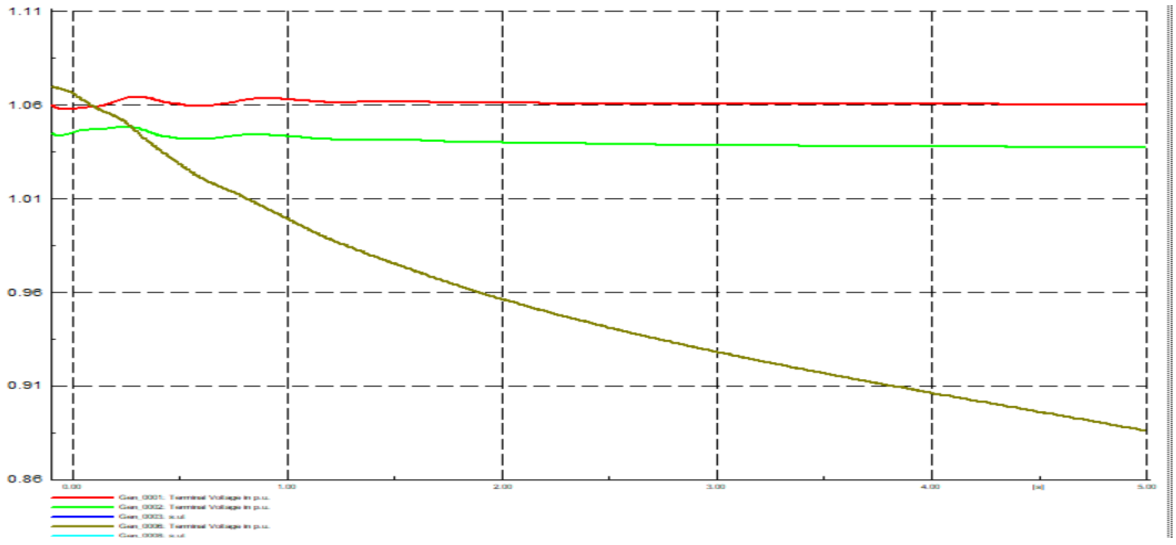

Figure 4.15: Scenario 1 Voltage plot for all gen

Voltage criteria for generator G6 has been violated which is below 0.9 pu of nominal voltage as seen from figure 4.15.

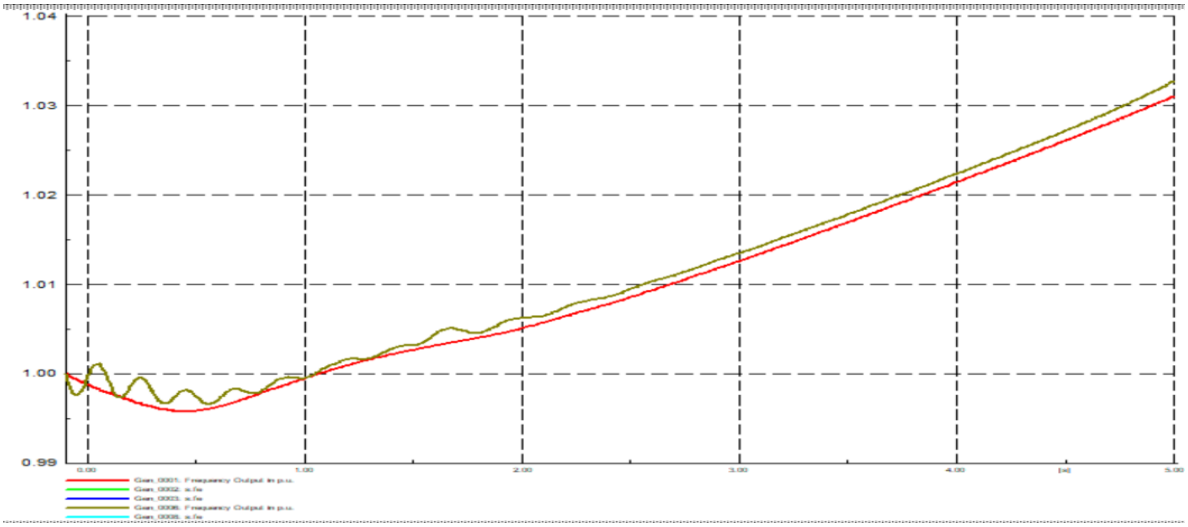

Figure 4.16:Frequency plot for scenario 2

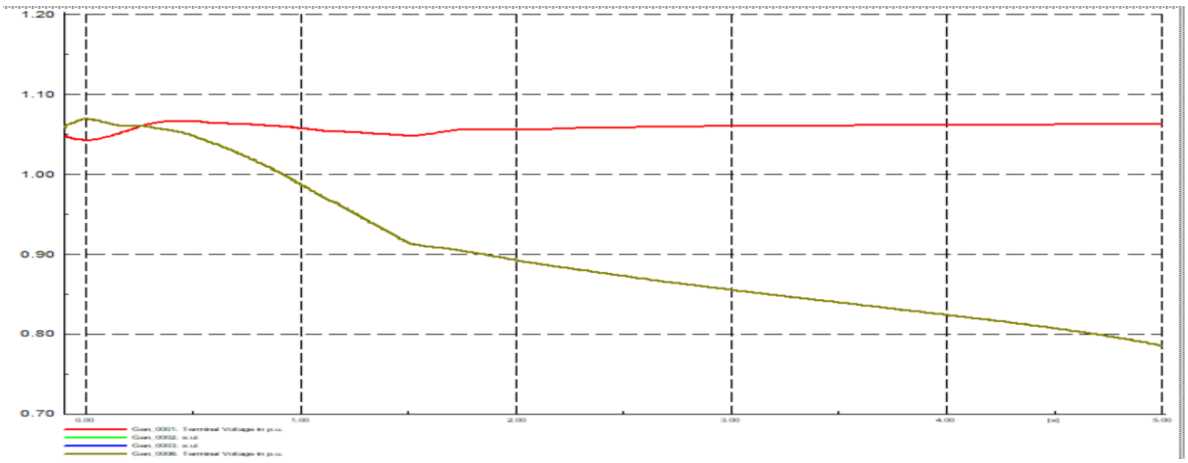

Figure 4.17: Voltage plot for scenario2

PV penetrated at bus 8 keeping gen 3 out of service with earlier contingencies and also load is reduced. Figure 36 shows clearly frequency rise violating the grid criteria with frequency 51.5 Hz with 100 MW PV penetration. Voltage of G6 is more reduced.

4.2.2 Heavy load and both temporary and permanent line outages

Figure 4.18 and 4.19 depicts the violation of grid frequency and voltage with the PV penetration when contingencies i.e. line to ground fault at bus1 and 3-phase short circuit fault at line 2-4 are applied for t=0.2 to 0.4 sec. 140 MW PV is penetrated at bus 8.

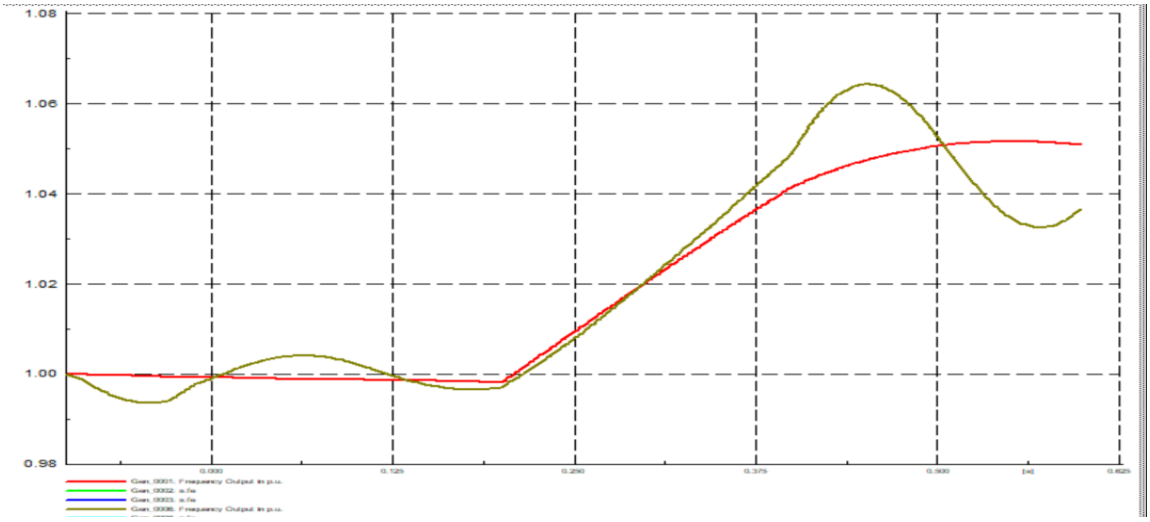

Figure 4.18: frequency(pu) of G1 & G6

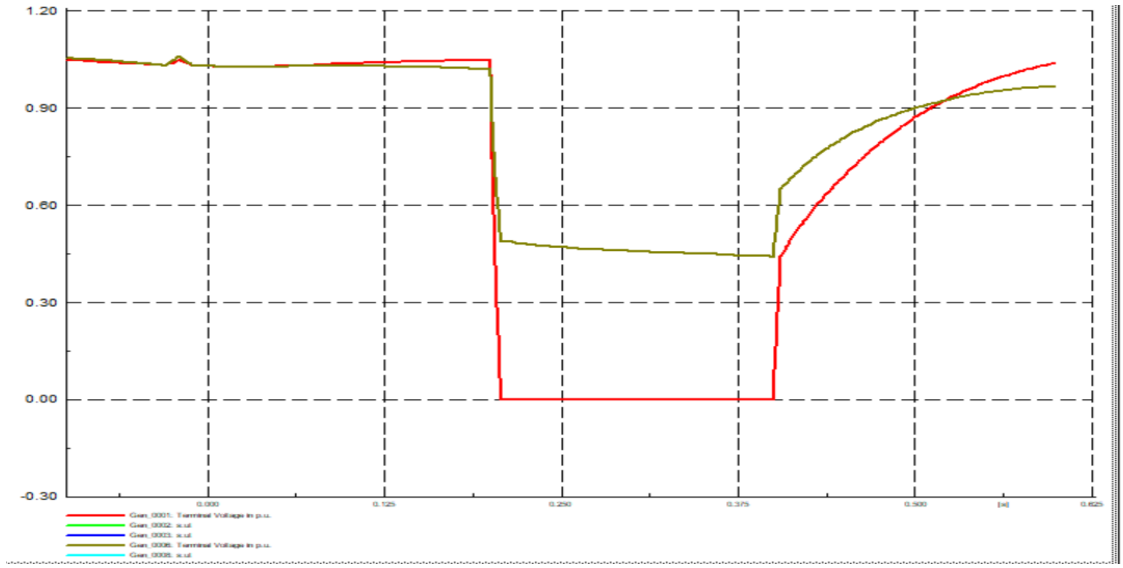

Figure 4.19: Voltage(pu) of G1 & G6

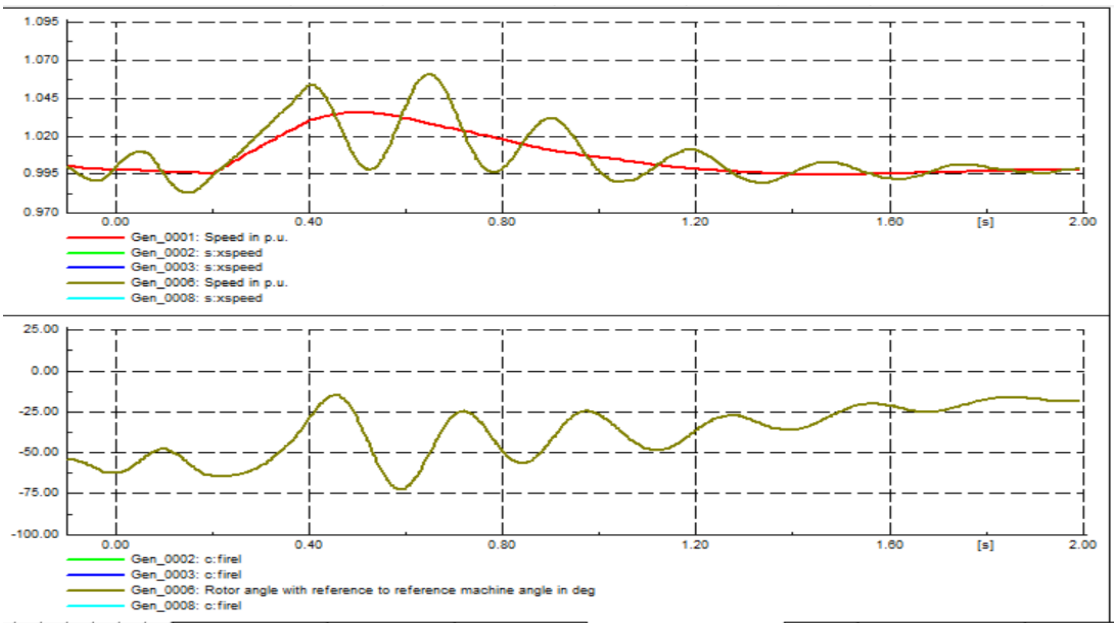

Figure 4.20 : frequency(pu) response with both PV & BESS

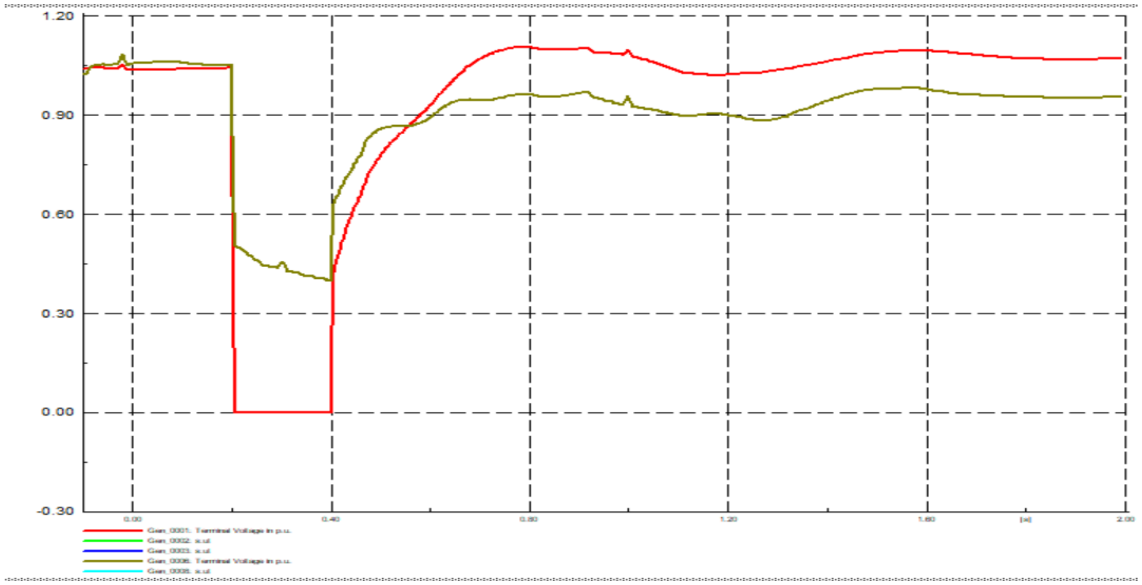

Figure 4.21: Voltage(pu) response with both PV & BESS

From figure 4.20 and 4.21, it is observed that the frequency and voltage of generator 1 & 6 under study are fully compliant with the NEM grid criteria. The frequency observed with 100 MW size of BESS installed at bus 6 is 0.996 pu i.e. 49.8 Hz for both generators and oscillations are also minimized. The voltages for G1 & G6 are 1.04 pu and 0.96

respectively. These findings demonstrate that, in the presence of disturbances, BESS enhances the voltage profile and speeds up system stabilization as in fig 4.23. Additionally, it has been shown that, in comparison to the absence of a BESS, the BESS significantly reduces the active power oscillations of the generator as shown below fig 4.22.

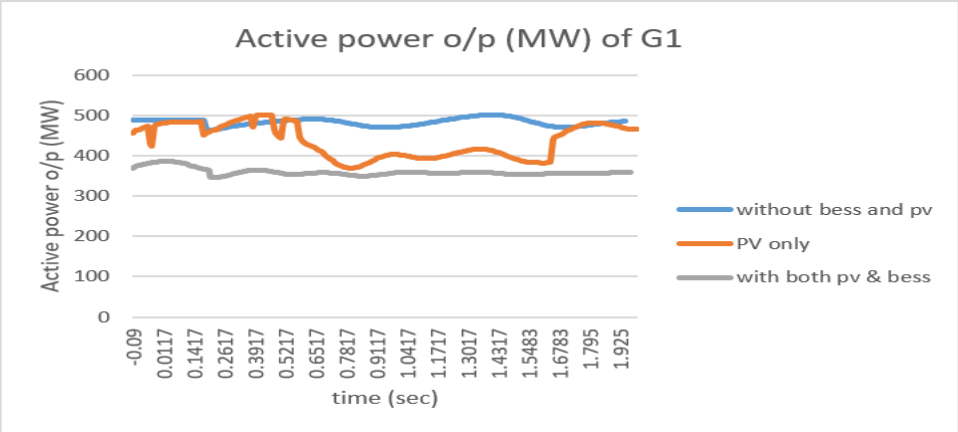

Figure 4.22:Active power o/p of G1

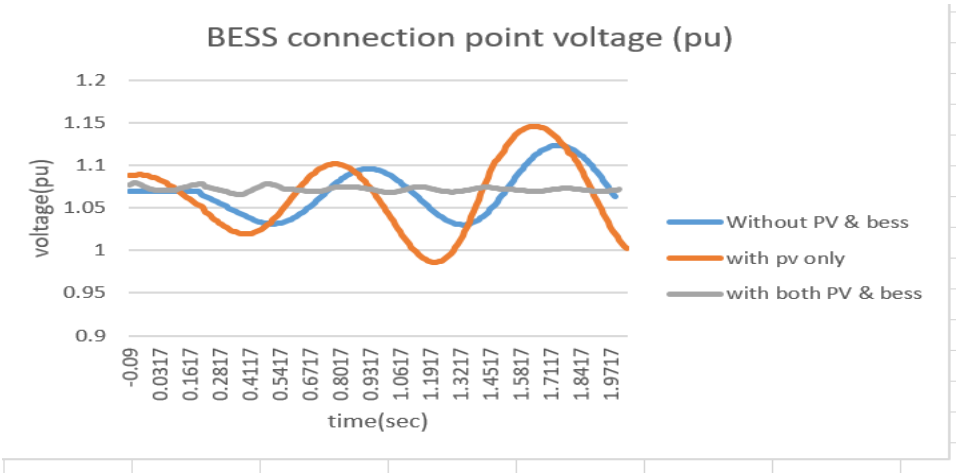

Figure 4.23:BESS Connection point voltage at different scenario

Finally analyzing all scenarios as shown in figure 4.24, the BESS size of 100 MVA installed at bus 6 maintains the frequency stability of the grid with PV penetration of nearly 30%.

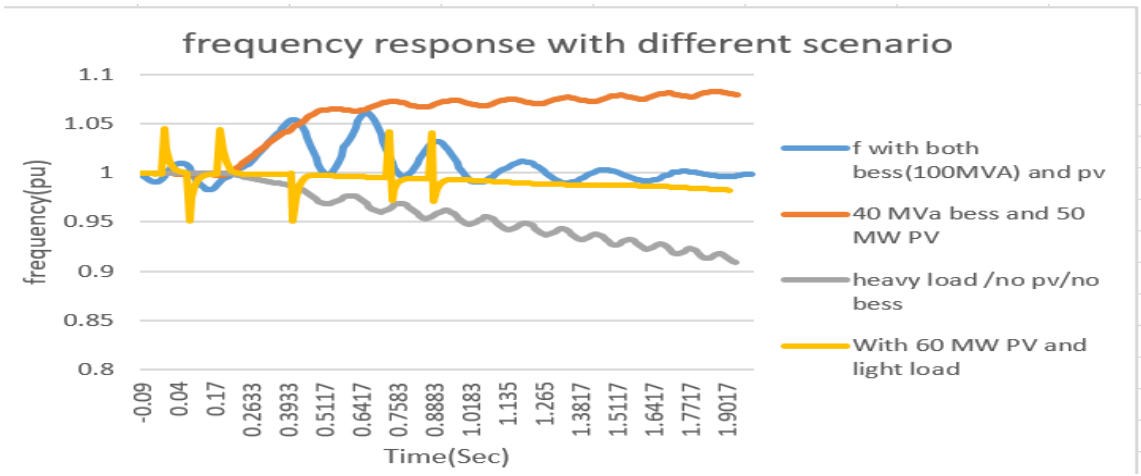

Figure 4.24: Frequency (pu)of G6 for different scenarios

4.2.3 BESS installation location & sizing

By deploying BESS at various buses, a comparative performance study of the location and converter size of the system is conducted. It has been discovered that all locations are not ideal for placing BESS because the grid cannot maintain frequency oscillations under criteria of the grid even with the rated BESS capacity. Thus, given the line outage and load event, it can be said that bus 6 is the best place for implementing BESS. The BESS is placed at three different locations and rotor angle vs. time is observed for generator 6 and it is found fast dampening of gen at bus 6 and hence it is concluded as optimal locations. Figure 4.25 demonstrates the rotor angle vs. time and f(pu) plot for BESS installed at different location and it is observed bus-06 is optimal. Also frequency plotted for the cases is shown below Figure 4.26.

Hence, a 100 MW of converter size is depicted from comparative performance analysis. Hence, BESS of size 100 MW is placed at bus 6 to provide required frequency support to the system.

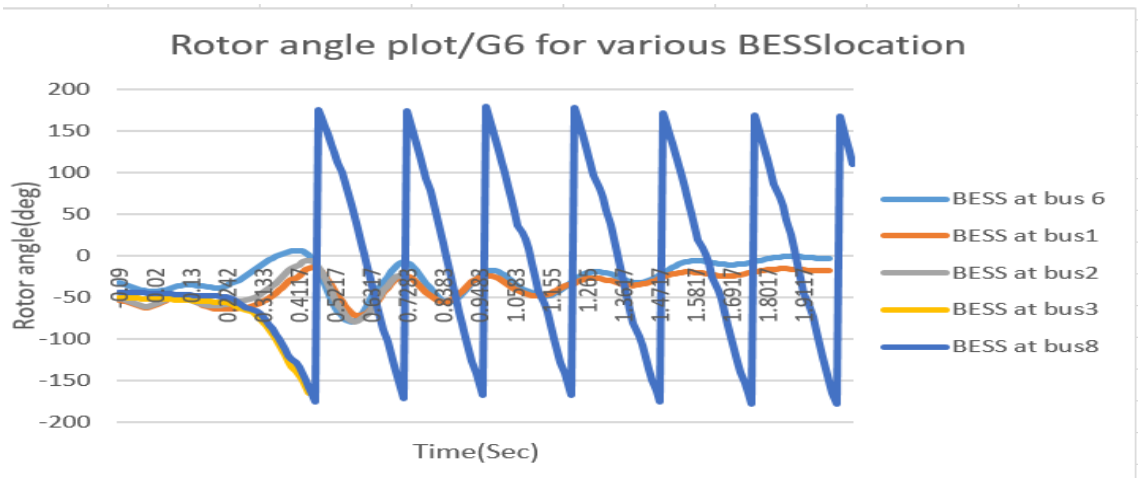

Figure 4.25: Rotor angle plot for various BESS location

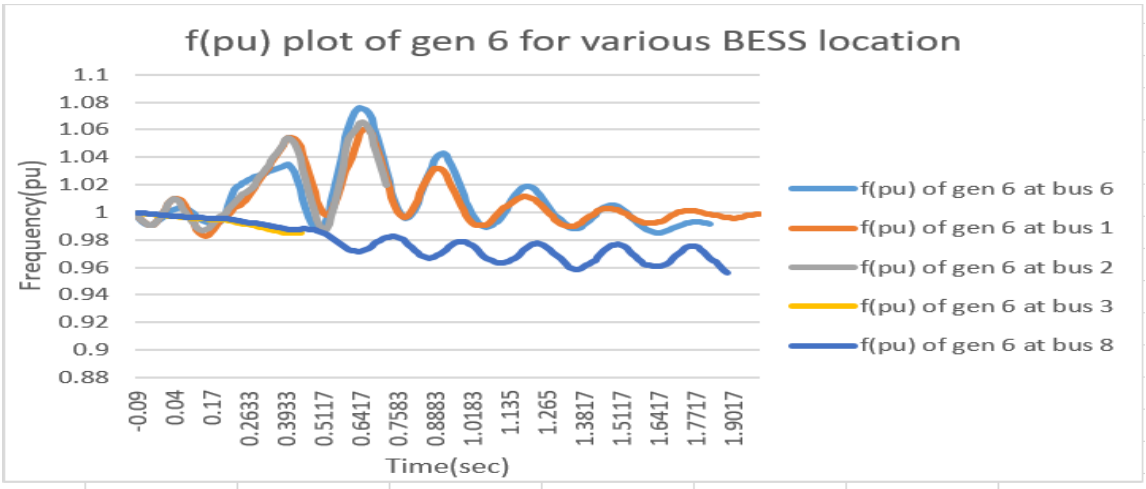

Figure 4.26: frequency plot for various BESS location

4.2.4 BESS Recharging

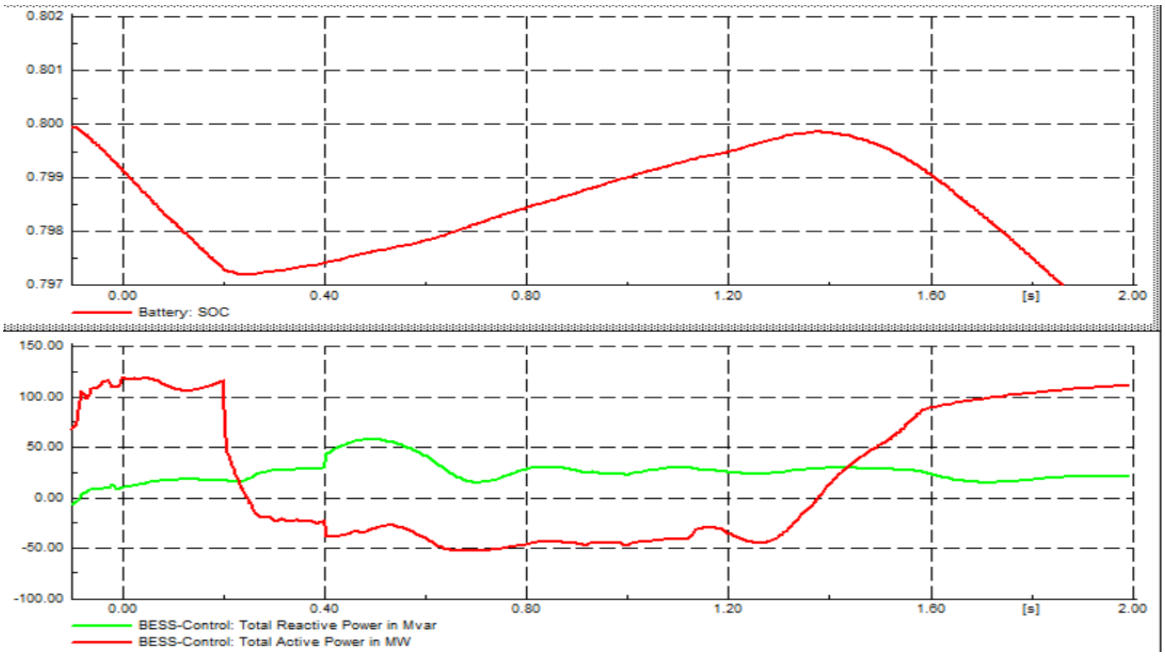

Figure 4.27 : SOC of Battery ;Active (MW)& reactive power(Mvar) provided by BESS Converter during contingencies

The self-discharging properties of the battery as well as the interchange of BESS power with the grid cause fluctuations in battery SOC. To guarantee that the cell is sufficiently charged to take part in power exchange anytime, a SOC recharge facility is necessary. The battery's state of charge variations during event intervals are displayed in Figure 4.25.

The BESS's real & virtual power transfer in transitory is presented in Figure 4.25. Because of narrower frequencies boundary control & higher precedence given to real power over virtual power, it can be observed that a significant quantity of active power as opposed to reactive power participates in frequency regulation.80 MW and 18 Mvar are the maximum exchanged value of active and reactive power of BESS respectively.

CHAPTER FIVE. CONCLUSIONS AND RECOMMENDATIONS

5.1 Conclusions

In this thesis work, a lead-lag droop controlled BESS is introduced to help the grid's frequency response and dampen oscillations caused due to high (>15%) PV integration. The simulation's output demonstrates that BESS offers enough dampening and improves the system's capacity to provide main frequency management with regard to power imbalances brought on by contingency occurrences. Theoretically sizing of BESS is done using inertia constant and droop control for 150 MW replacement of conventional generation with PV, 75 MW sizing of BESS is obtained. The optimal BESS location is found for both IEEE test systems by observing the faster dampening of oscillations from rotor angle Vs. time plot.

The analysis of two operating methods reveals that sustaining frequency within the grid defined peripheral depends critically on the power reserve of the generators in pre-fault state. However, because of the lack of sunlight, generators must run at higher output at peak times or at lower PV outputs. Grid fails to uphold NEM standards with 100MW of PV penetration.

When a 100 MW of PV is penetrated with temporary and permanent line outage and heavy load, it is observed that frequency of grid is violated i.e. variations in the frequencies of G1 & G2 are extremely oscillating and exceed the required grid limit by 1.0204 (51.02 Hz; G1) and 1.0246pu (51.23 Hz; G2) respectively. With the addition of 50 MW BESS at bus 7 of IEEE 9 bus system, the frequency of G1 and G2 are under NEM 2% grid criteria i.e. 50.365 Hz & 50.487 respectively.

Also for IEEE 14 bus system frequency rise violating the grid criteria with frequency 51.5 Hz with 140 MW PV penetration. The frequency observed with 100 MW size of BESS installed at bus 6 is 0.996 pu i.e. 49.8 Hz for both generators and oscillations are also minimized.

The optimal Sizing and location is also achieved through scenario and comparative performance analysis in this research. Battery storage also acts promptly, charging and

discharging the battery in response to voltage peaks and valleys and taking the initiative to keep the power system's stable voltage source constant. Additionally, compared to a system without a BESS, BESS minimizes active power and voltage oscillations more quickly. Therefore, BESS may be used to control the grid's voltage and frequency as well as to reduce the detrimental inertial effects of PV generation.

5.2 Recommendations

There is sufficient room for additional breakthroughs in BESS control approaches in further study work since it has been found that the regulation strategies used to manage BESS power output have a major influence on its performance. Future research will concentrate on grid-based optimization for techno-economic evaluation.

- Throughout the BESS lifespan, BESS experiences frequent fast charging and discharging, which raises the impedance of battery cells and causes battery deterioration. Future research will pay more attention to techno-economic assessment through optimization during grid service in order to achieve this goal.
- The size and placement of the battery play a significant role in ensuring that the BESS is used to its fullest potential while still providing the essential services. Therefore, to find the best size and location of BESS installation for maximal techno-economic value, optimization methodologies including “stochastic, heuristic/meta-heuristic, and evolutionary computing techniques” might be applied.
- Peak or average value of solar power is only taken for analysis here. In future work validation of the fluctuating nature of PV into analysis, using some probabilistic analysis is recommended.

REFERENCES

[1] S. Impram and B. Oral, "Challenges of renewable energy penetration on power system flexibility," *Energy Strategy Reviews,* vol. 31, p. 100539, 2020.

[2] A. K. a. J. S. U. Datta, "The relevance of large-scale Battery Energy Storage system for providing primary frequency control with increased Wind energy penetration," *Journal of Energy Storage,* vol. 23, pp. 9-18, 2019.

[3] U. Datta, A. Kalam and J. Shi, "BESS control for mitigating PV penetration Impact and State of Charge recovery," *IEEE Transaction on sustainable energy,* vol. 11, pp. 746-757, 2020.

[4] J. S. a. A. K. U. Datta, "Primary frequency control of a microgrid with integrated dynamic sectional droop and fuzzy based pitch angle control," *International Journal of Electrical Power & Energy System,* vol. 11, pp. 248-259, 2019.

[5] U. datta, A. Kalam and J. Shi, "Battery Energy Storage system to stablize transient voltage and frequency and enhance power export capability," *IEEE transactions on power system,* 2018.

[6] A. K. a. J. S. U. Datta, "Smart control of BESS in PV integrated EV charging station for reducing transformer overloading and providing battery-to-grid," *Journal of Energy Storage,* vol. 28, p. 101224, 2020.

[7] v. Knap, S. K. Chaudhary and D. I. Stroe, "Sizing of Energy storage System for Grid Inertial Response and primary Frequency Reserve," *IEEE transactions on Power System,* vol. 31, no. 5, 2016.

[8] A. Jaiswal, "Lithium-ion battery based renewable energy solution for off-grid," *Renewable and Sustainable Energy,* vol. 72, p. 922 – 934, 2017.

[9] X. L. a. S. Wang, "A review on energy management, operation control and application method methods for grid battery energy storage systems," *CSEE Journal of Power and Energy Systems,* 2019.

[10] A. L. J. a. N. J. P. G. Oriti, "“Power-electronics-based energy mangement system with storage," *IEEE Transactions on Power Electronics,* vol. 31, pp. 452-460, 2016.

[11] B. K. J. M. L. C. A. A. a. Y. L. P. F. Ribeiro, "Energy storage system for advanced power system application," *Proceedings of the IEEE,* vol. 89, pp. 1744-1756, 2001.

[12] B. Dunn, H. Kamath and J. Tarascon, "Electrical energy storage for the grid: A battery of Choices," *Science,* vol. 334, no. 6058, pp. 928-35, 2011.

[13] H. Zhao, Q. Wu and S. Hu, "Review of energy storage system for wind power integration support," *Applied energy,* vol. 137, pp. 545-53, 2015.

[14] J. Baker, "New technology and possible advances in energy storage," *Energy policy,* vol. 36, no. 12, pp. 4368-73, 2008.

[15] K. D. a. J. Østergaard, "Battery energy storage technology for power system-An overview," *Electric Power Systems Research,* vol. 79, no. 4, pp. 511-20, 2009.

[16] A. D. a. B. M. G. J. May, "Lead batteries for utility energy storage : A Review," *Journal of Energy Storage,* vol. 15, pp. 145-157, 2018.

[17] M. S. Whittingham, "“History, evolution, and future status of energy storage,”," *proceedings of IEEE,* vol. 100, pp. 1518-34, 2012.

[18] T. S. a. A. B. M. Ceylan, "A novel lithium-ion-polymer battery model for hybrid/electric vehicles," *International Symposium on Industrial Electronics (ISIE),* p. 366, 2014.

[19] H. Bayat and A. Yazdani, "A hybrid mmc-based photovoltaic and battery energy storage system," *IEEE Power and Energy Technology Systems Journal,* vol. 6, pp. 32-40, 2019.

[20] M. Di Piazza, M. Luna and G. Tona, "“Improving grid integration of hybrid PV-storage systems through a suitable energy management strategy," *IEEE Transaction on Industrial Application,* vol. 55, pp. 60-68, 2019.

[21] A. G. P. a. S. A. P. S. I. Nanou, "A generic modelof two-stage grid-connected PV systems with primary frequency response and inertia emulation," *Electric Power Systems Research,* Vols. 186-196, p. 127, 2015.

[22] B. C. a. R. B. V. A. K. Pappu, "Implementing frequency regulation in solar PV plant," *North American Power Symposium 2010,* pp. 1-6, 2010.

[23] M. R. Aghamohammadi and H. Abdolahinia, "A new approach for optimal sizing of BESS primary frequency control of islanded microgrid," *International Journal of Electrical Power and Energy Systems,* vol. 54, pp. 325-333, 2014.

[24] M. F. M. A. a. E. F. El-Saadany, "Implementing virtual inertia in dfig-based wind power generation," *IEEE Transactions on Power Systems,* vol. 28, p. 1373–1384, 2013.

[25] Y. I. A. U. N. U. T. S. a. A. Y. S. A. M. Howlader, "A robust h∞ controller based frequency control approach using the wind-battery strategy in small power system," *International Journal of Electrical power & energy system,* vol. 58, 2014.

[26] C. Zhou, K. Qian and M. Allan, "Modeling of the cost of ev battery wear due to v2g application in power systems," *IEEE Transactions on Energy Conversion,* vol. 26, p. 1041–1050, 2011.

[27] M. Murnane and A. and Ghazel, "A Closer Look at State of Charge (SOC) and State of Health(SOH)Estimation technique for battries," [Online]. Available: https://www.analog.com/media/en/technical-documentation/technical-articles/a-closer-look-at-state-of-charge-and-state-health-estimation-techniques.pdf. [Accessed 11 12 2018].

[28] E. K. V. S. M. J. S. D. I. &. T. R. Thorbergsson, "Primary Frequency Regulation with Li-Ion Battery Based Energy Storage System - Evaluation and Comparison of Different Control Strategies," in *Proceedings of the 35th International Telecommunications Energy Conference 'Smart Power and Efficiency',INTELEC 2013*, Aalborg, Denmark , 2013.

[29] AEMC, "The Frequency Operating Standard," *Online,* 2020.

[30] P. Breeze and m. l. k. Joe Hayton, *Developing a Control Strategy for frequency stability using BESS in Microgrid,* Power System Energy Storage Technologies, 2018.

[31] S. Alhejaj and F. G. Longatt, "Investigation on Grid-Scale BESS Providing Inertial Response Support," *IEEE,* 2016.

[32] M. Y. G. Nuhic, " Battery Energy Storage System Modelling in DIgSILENT PowerFactory," in *Modelling and Simulation of Power Electronic Converter Dominated Power Systems in PowerFactory*, Switzerland, Springer, 2021, pp. 177-192.

[33] D. GmbH, "PV System," 2017.

[34] A. Anuar, M. Wahab and S. Arshad, "Transient stability for IEEE 14 bus power system using power worldsimulator," in *Journal of Physics: Conference series*, Malayasia, 2020.

[35] S. Akkari, J. Dai and M. Petit, "Intereactions between Voltage droop and frequency droop control for multi terminal HVDC system," *IET G,T&D,* vol. 10, no. 6, p. 1345=1352, 2016.

[36] DigSiLENT, "DigSilent Powerfactory," 2017.

[37] D. Greenwood, K. Lim and P. Lyons, "Frequency response services designed for energy storage," *Applied Engineering,* vol. 203, pp. 115-127, 2017.

[38] L. Quingsheng, T. Yibin and Z. Yu, "Simulation and modelling for Active distribution network BESS system in DigSilent," *ScienceDirect,* 2022.

[39] A. Turk, M. Sandelic, G. Noto and K. S. Chaudhary, "Primary frequency regulation supported by battery storage systems in power system dominated by renewable energy sources," *IET,* vol. 2019, no. 18, pp. 4986-4990, 2018.

[40] D. C. a. C. O. Alexandre Oudalov, "Optimizing a Battery Energy Storage System For Primary Frequency Control," *IEEE TRANSACTIONS ON POWER SYSTEMS,* vol. 22, no. 03, 2007.

[41] J. Fradley, R. Preece and M. Barnes, "The Influence of Network Factors on Frequency Stability," *IEEE TRANSACTIONS ON POWER SYSTEMS,* vol. 34, no. 04, 2020.

[42] F. G. Longatt and J. Torres, Advanced Smart Grid Functionalities Based on Power Factory, S Cham, Switzerland: pringer International Publishing:, 2018.

[43] G. Delille, B. François and G. Malarange, " Dynamic frequency control support by energy storage to reduce the impact of wind and solar generation on isolated power system's inertia.," *IEEE Trans. Sustain. Energy*, vol. 3, p. 931–939, 2012.

[44] F. Gonzalez-Longatt and J. Torres, Power Factory Applications for Power System Analysis, Cham, Switzerland: Springer, 2014.

APPENDIX A: System Model in Power Factory

The whole system model in Power Factory is presented in Figure A.1.

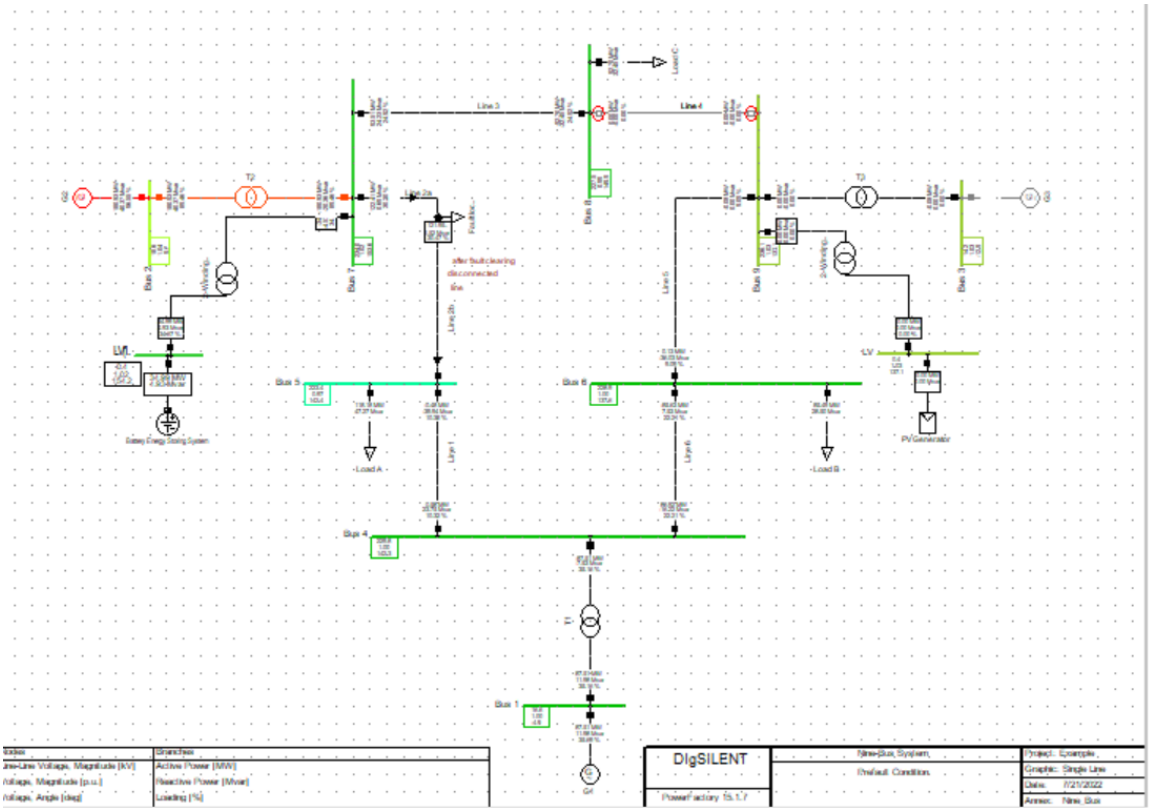

Figure A.1: The whole system model in Power factory

BESS controller:

The BESS control strategy is developed with the purpose to regulate the system frequency at the normal value in the system containing the RESs. This BESS consists of various elements and controllers as shown in Figure A.2.

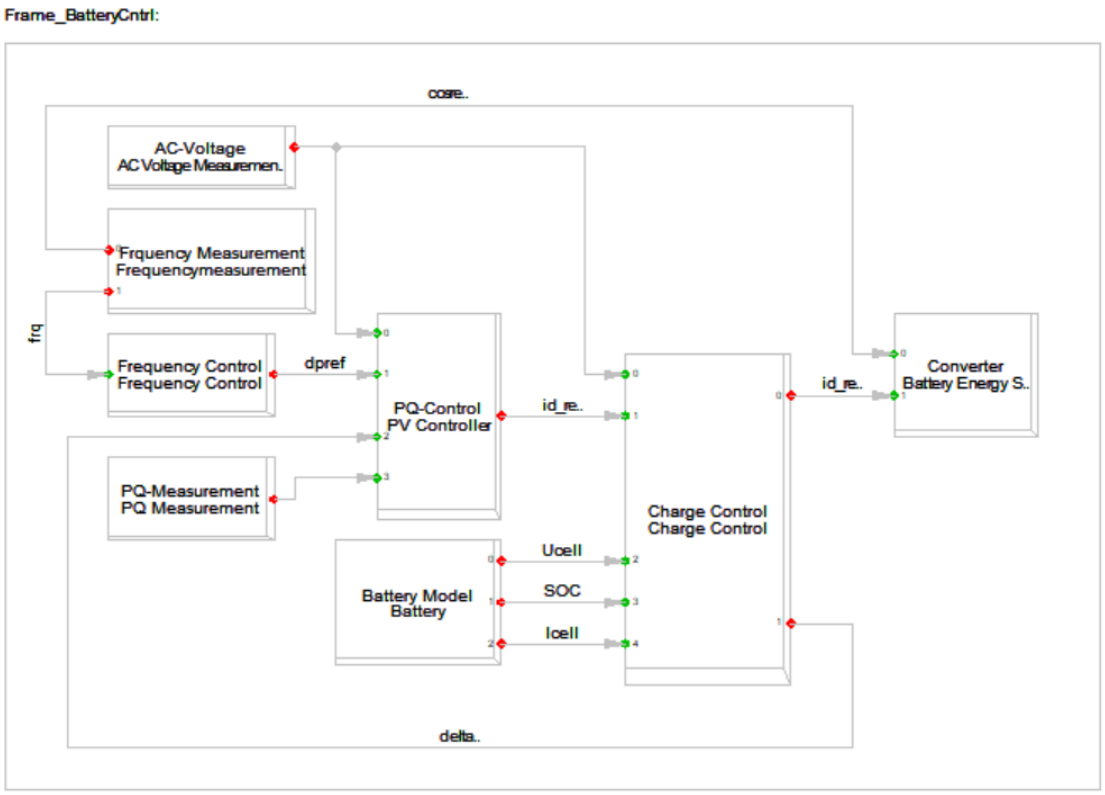

Figure A.2: Schematic diagram of BESS frame

PLL: This is used to track the frequency using the measured input voltage signal in grid.

Frequency controller: This is modelled as shown in Figure A.3, where it starts by comparing the measured frequency from PLL block to the frequency reference set as 1 [pu] equivalent to 50 [Hz]. The output signal leads to deadband block with a gain of 0.004 [pu] identical to 20 mHz. The output information from deadband block leads to droop block with a gain of 0.004 [pu] identical to 200 [mHz] of frequency deviation. This means that if

the frequency deviation is equal or above 200 [mHz], then the BESS will activate the full power. The offset block compensate the output dpref in case it is not equal to zero.

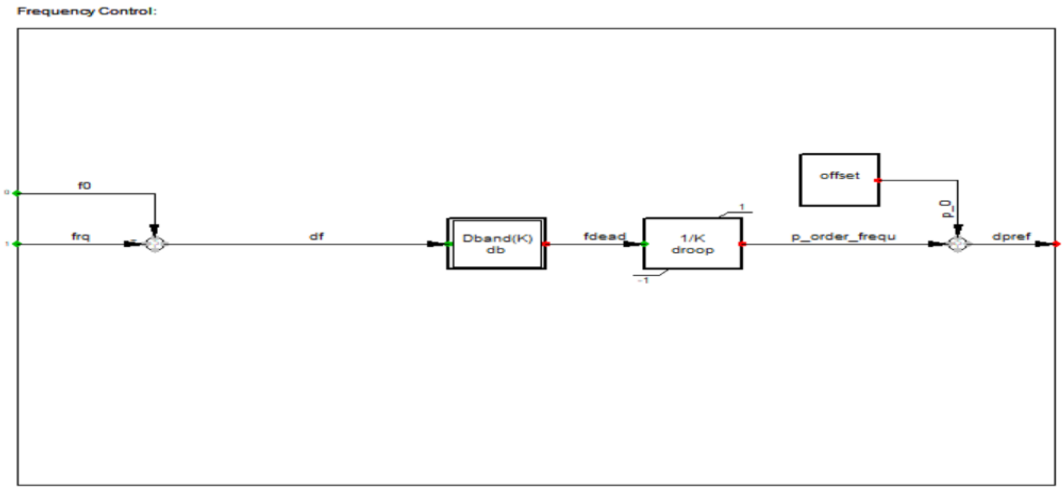

Figure A.3 :Schematic diagram of Frequency Controller

PQ controller: This controller includes the active power and voltage control as presented in Figure A.4. For the active power control, the dpref from frequency control is first compared to the measured active power in grid, the output signal is adjusted by PI control block which thereby generate the active current idref . In addition, the voltage is adjusted by comparing the measured voltage and the voltage reference and then output the reactive current signal iqref.

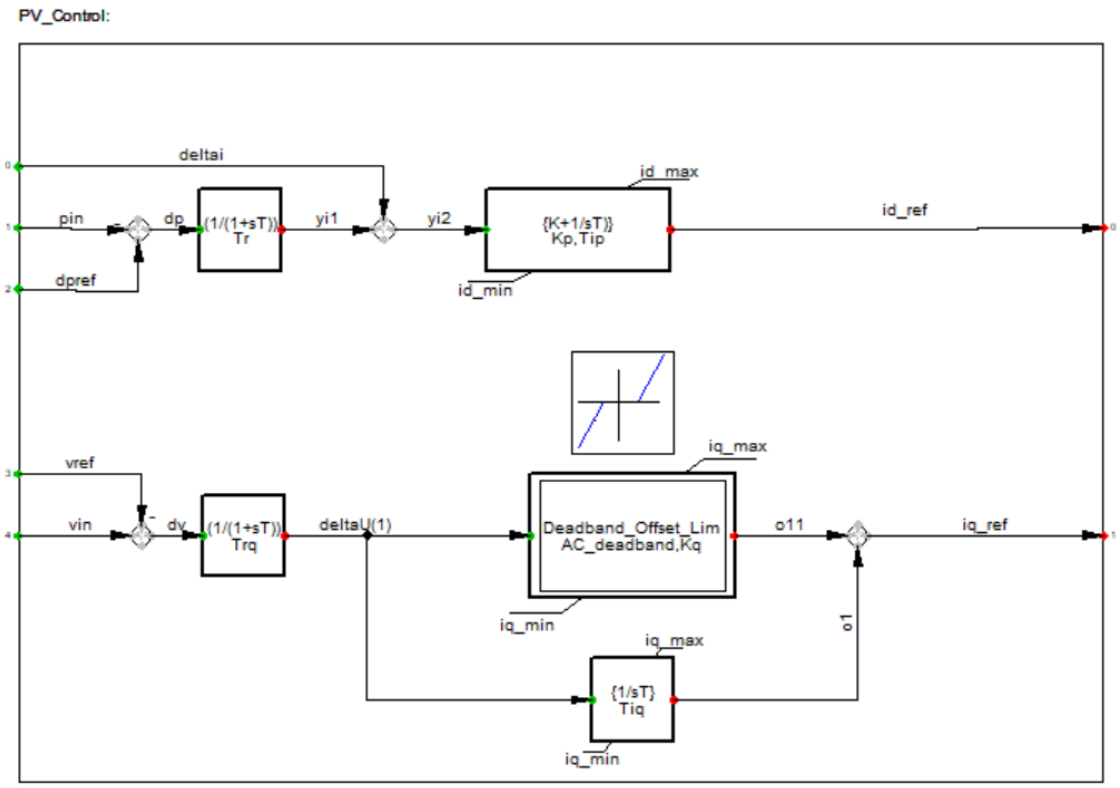

Figure A.4: Schematic for PQ model

Table A.1: PQ controller settings

Parameter	Value
Tr(Filter time constant, active path [s])	0.01
Trq(Filter time constant, reactive path [s])	0.1
Kp(Proportional gain-id-PI-controller [pu])	2.
Tip(Integrator time constant -id-PI-control [s])	0.2
AC deadband for proportional gain[pu])	0.
Kq(Proportional gain for AC-volt support [pu])	1.

Tiq(Integrator time constant iq-I-control [a])	0.002
idmin(Min discharging current [pu])	-0.4
iqmin(Min reactive current [pu])	-1.
idmax(Max charging current [pu])	1.
iqmax(Max reactive current [pu])	1.

Charge controller: This controller receives the output current signals from PQ controller together with the information about the battery state of charge (SOC) from battery model, it decides whether the battery charges or discharges depending on the frequency condition in grid. The schematic for charge controller is given in Figure A.5 and parameter settings in table A.2.

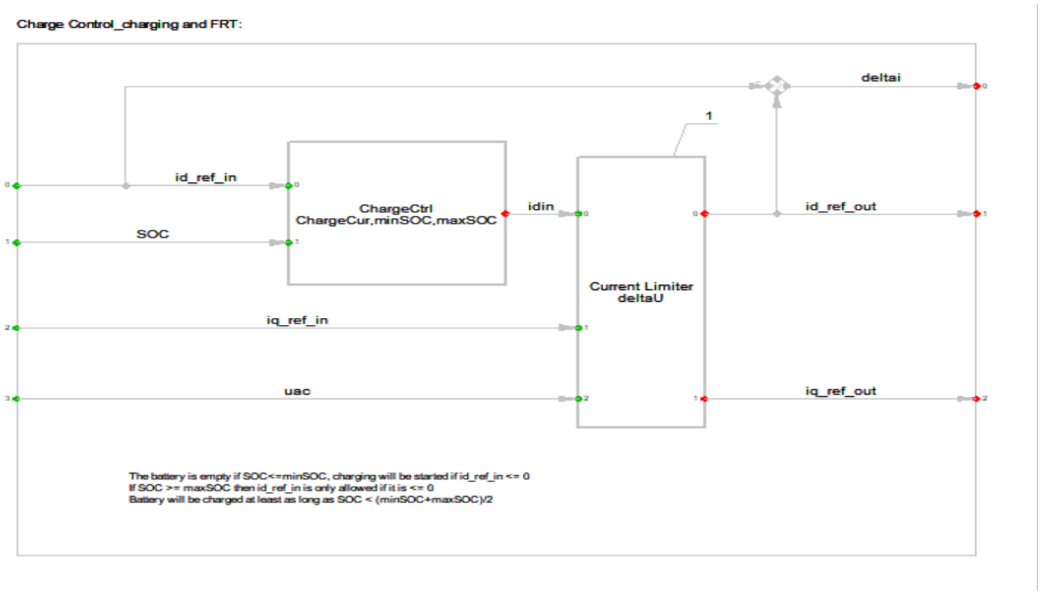

Figure A.5 : Charge control model

Table A.2: Charging control

Parameter	Value
Min charging current[pu]	0.8
Min SOC[pu]	0.1
Max SOC[pu]	0.9
Max Abs Cur[pu]	1

Battery model: This model is provided with a DC-current signal, and this is processed through different blocks for integrator and gain so as it generates the proper output DC-voltage, the SOC and DC-cell voltage as shown in Figure.

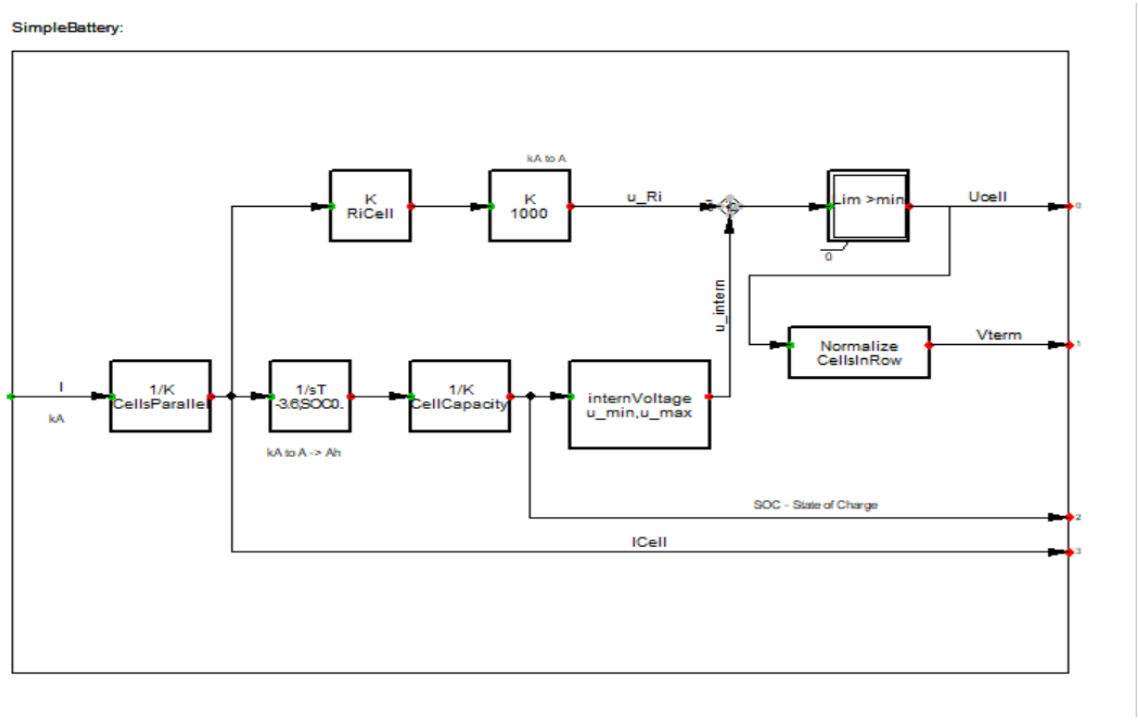

Figure A.6: Battery model

Table A.3 : Battery parameters

Parameter	Value
SOCo (Initialization) [pu]	0.8
Cell capacity per cell [Ah]	80.
Vmin(Voltage of empty cell) [V]	12.
Vmax Voltage of full cell [V]	13.85
Parallel cells	60.
Cells in series	65.
Vnom Nominal voltage of source [kV]	0.9
Ri Intern resistance per cell [Ω]	0.001

Table A.4: BESS controller settings

Controller/Component	**Parameters**
Frequency controller	dead band- 0.0004, droop setting: R=0.001
Voltage controller	dead band- 0.1, droop setting: R=1 P controller: Kp=1, Ki=1, Tip=0.04, ymin=id−min =iq−min= -0.7pu
Q controller	Kp=0.25, Ki=0.25, Tiq=1, ymax=id−max =iq−max= 1pu,

Current controller	Kd= Kq= Kid= Kiq=1, Td= Tq=0.01
Battery parameter:	Initial SOC=80%, capacity/Cell (Ah)=12, no. of parallel cell=20, nominal voltage=0.9kV, SOCmin=0.2, SOCmax=1.
PI controller	Tp=0.01, Tq=0.02, Kd=Kq=1, Tid=4, Tiq=4, id−max=iq−max=1, id−min=iq−min=-1.
PI-lead controller	Tp=0.01, Tq=0.02, Tb1=Tb2=1, Ta1=Ta2=0.5, Kd=Kq=1, Tid=4, Tiq=4, id−max=1, id−min=iq−min=-1.
Lead-lag controller	T=6; Tz1=1, Tp1=0.5, Tz2=4, Tp2=15, Tz3=1, Tp3=0.5, Tz4=4, Tp4=15, KP =KQ=5, id−max=iq−max=1, id−min=iq−min=-1.

Photo-voltaic Model: This contains a dsl model for PV model. The used setting in this model are presented in table A.5.

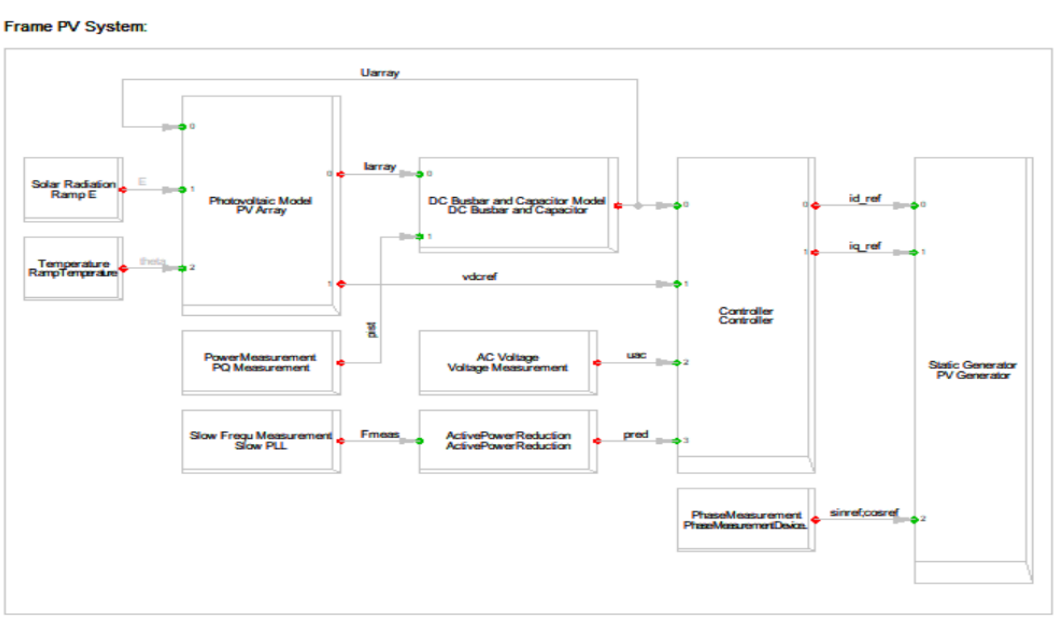

Figure A.7: PV system model frame

Table A.5: PV array settings

Parameter	Value
VO(Open-circuit voltage of module at STC [V])	43.8
VMP P (MPP voltage of module at STC) [V]	35
IMP P (MPP current of module at STC) [A]	4.58
Isc (Short circuit current of module at STC) [A]	5
Temperature correction factor(Voltage) [1/K]	−0.0039
Temperature correction factor(Current) [1/K]	0.0004
Time constant of module [s]	0
nseries(Number of modules in series)	20
nparallel(Number of modules in parallel)	140

Controller: This controller model is used for voltage and reactive power control. The controller settings can be seen in Table A.6.

Measurement solar radiation: This block contains the imported solar radiation file with radiation profile.

Static generator: This plays a role as an inverter.

AC voltage: This is used to measure the ac voltage used to detect the fault

PLL: This is used to calculate the frequency form the measured voltage in grid.

PQ measurement: This measures the active and reactive power in grid, which are needed for control feedback

Table A.6: Controller settings

Parameter	Value
p(Gain)	0.005
ip(Integration time constant)[s]	0.03
r(Measurement Delay[s]	0.001
mpp (Time Delay MPP-Tracking)[s]	5
deadband for dynamic AC voltage support[pu]	0.1
F RT (Gain for dynamic AC voltage support)	2
dmin Minimum active current limit[pu]	0
min allowed DC-voltage[V]	200

qmin(Minimum reactive current limit[pu])	−1
dmax(Maximum active current limit[pu])	1
qmax(Maximum reactive current limit[pu])	1
axAbsCur (Maximum allowed absolute current[pu])	1
axIqMax.abs (reactive current in normal operation) [pu]	1

APPENDIX B: Data of Modified IEEE 9 & 14 bus systems

Data for IEEE 9 Bus System:

Table B.1: Generator data for IEEE 9 bus system

Generator	1	2	3
Rated MVA	247.5	192	128
kV	16.5	18.0	13.8
Power factor	1.0	0.85	0.85
Type	Hydro	Steam	Coal
Speed	180 r/min	3600 r/min	3600 r/min
x_d	0.1460	0.8958	1.3125
x'_d	0.0608	0.1198	0.1813
x_q	0.0969	0.8645	1.2578
X'_q	0.0969	0.1969	0.25
x_l	0.0336	0.0521	0.0742
T'_{d0}	8.96	6.00	5.89
T'_{q0}	0	0.535	0.6
Stored Energy @ rated speed	2364 MWS	640 MWS	301 MWS

-

Table B.2: Network Data for IEEE 9 bus system

Line	R	X	G	B
4-5	0.01	0.085	1.3652	-11.6041
4-6	0.0170	0.0920	1.9422	-10.5107
5-7	0.0320	0.1610	1.1876	-5.9751
6-9	0.0390	0.17	1.282	-5.5882
7-8	0.0085	0.0720	1.6171	-13.698
8-9	0.0119	0.1008	1.1551	-9.7843
T1	0	0.1184	0	-8.4459
T2	0	0.1813	0	-5.4855
T3	0	0.2399	0	-4.1684

Table B.3: Generator data for IEEE 14 bus system

Generator	Bus Type	Voltage (KV)	Voltage(pu)	MVA(min.)	MVA(max.)
Gen 001	Slack	22	1.060	NA	NA
Gen 002	PV	13.8	1.045	-40.0	50.0
Gen 003	PV	13.8	1.010	0.0	40.0
Gen 006	PV	13.8	1.070	-6.0	24.0
Gen 008	PV	13.8	1.090	-6.0	24.0

Table B.4: Data of transformers based on 100 MVA

Transformer	HV (KV)	LV (KV)	Capacity (MVA)	r in pu	x in pu
Trf 4-7	220	132	100	0.0	0.20912
Trf 4-9	220	132	100	0.0	0.55618
Trf 5-6	220	132	100	0.0	0.25202
Trf 8-LV (PV)	132	0.4	200	0.0	0.03
Trf6-LV(BESS)	132	0.4	200	0.0	0.03

Table B.5: Data of lines based on 100 MVA

From Bus	To Bus	r in p.u.	x in p.u.	$Q_{c/2}$ in p.u.	b in p.u.
1	2	0.01938	0.05917	0.0264	0.0528
1	5	0.05403	0.22304	0.0246	0.0492
2	3	0.04699	0.19797	0.0219	0.0438
2	4	0.05811	0.17632	0.0187	0.0374
2	5	0.05695	0.17388	0.0170	0.0340
3	4	0.06701	0.17103	0.0173	0.0346
4	5	0.01335	0.04211	0.0064	0.0128
6	11	0.09498	0.19890	0.0000	0.0000
6	12	0.12291	0.25581	0.0000	0.0000

6	13	0.06615	0.13027	0.0000	0.0000
9	10	0.03181	0.08450	0.0000	0.0000
9	14	0.12711	0.27038	0.0000	0.0000
10	11	0.08205	0.19207	0.0000	0.0000
12	13	0.22092	0.19988	0.0000	0.0000
13	14	0.17093	0.34802	0.0000	0.0000

Originality Report:

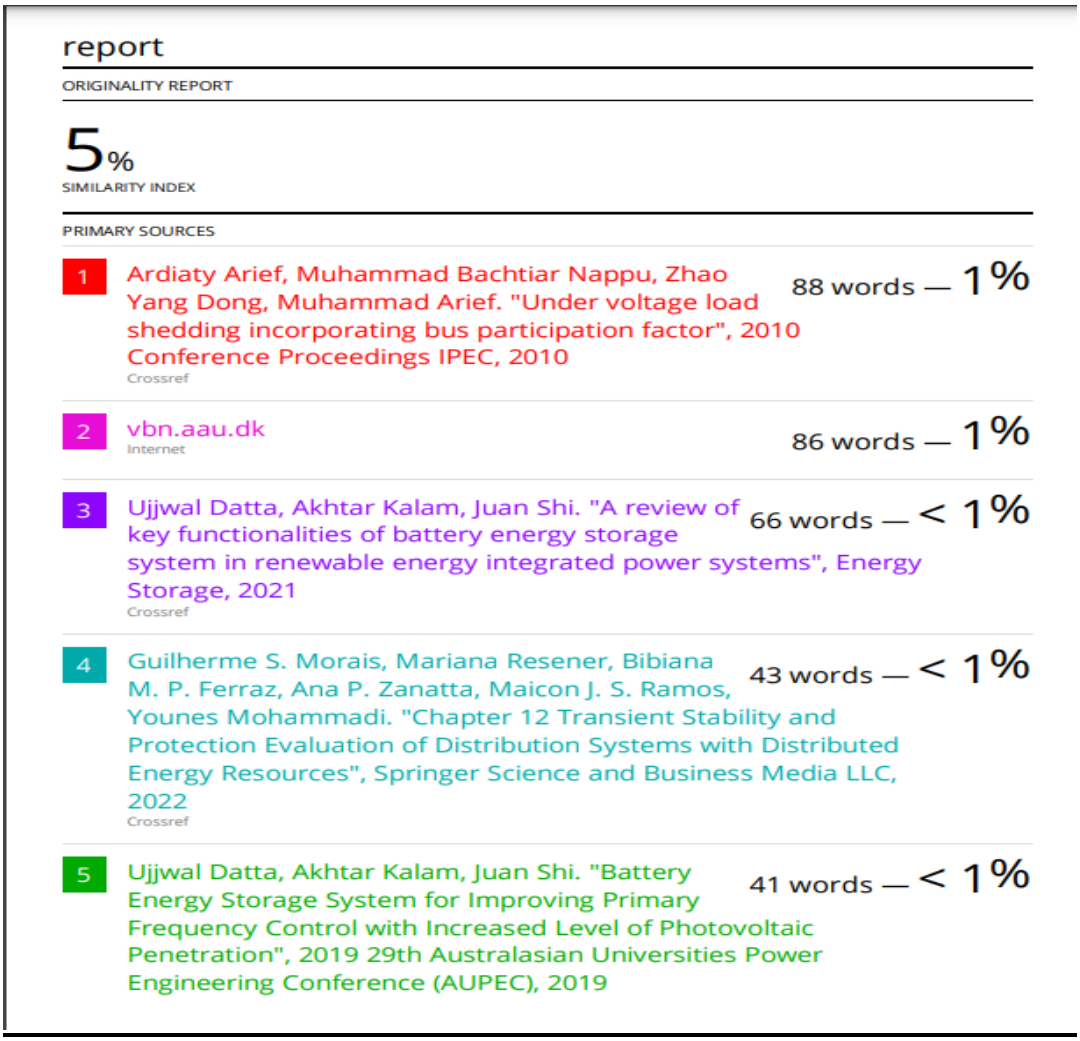

report

ORIGINALITY REPORT

5%
SIMILARITY INDEX

PRIMARY SOURCES

1 Ardiaty Arief, Muhammad Bachtiar Nappu, Zhao Yang Dong, Muhammad Arief. "Under voltage load shedding incorporating bus participation factor", 2010 Conference Proceedings IPEC, 2010 — 88 words — 1%
Crossref

2 vbn.aau.dk — 86 words — 1%
Internet

3 Ujjwal Datta, Akhtar Kalam, Juan Shi. "A review of key functionalities of battery energy storage system in renewable energy integrated power systems", Energy Storage, 2021 — 66 words — < 1%
Crossref

4 Guilherme S. Morais, Mariana Resener, Bibiana M. P. Ferraz, Ana P. Zanatta, Maicon J. S. Ramos, Younes Mohammadi. "Chapter 12 Transient Stability and Protection Evaluation of Distribution Systems with Distributed Energy Resources", Springer Science and Business Media LLC, 2022 — 43 words — < 1%
Crossref

5 Ujjwal Datta, Akhtar Kalam, Juan Shi. "Battery Energy Storage System for Improving Primary Frequency Control with Increased Level of Photovoltaic Penetration", 2019 29th Australasian Universities Power Engineering Conference (AUPEC), 2019 — 41 words — < 1%

Crossref

6	ir.canterbury.ac.nz Internet	36 words — < 1%
7	Z R Renaldhy, A R Hutajulu, F Husnayain, D R Aryani, A R utomo. "Dynamic simulation of a hybrid PV/Wind/Diesel system using power factory", IOP Conference Series: Earth and Environmental Science, 2020 Crossref	33 words — < 1%
8	vuir.vu.edu.au Internet	28 words — < 1%
9	paduaresearch.cab.unipd.it Internet	25 words — < 1%
10	www.mdpi.com Internet	25 words — < 1%
11	creativecommons.org Internet	21 words — < 1%
12	kashanu.ac.ir Internet	19 words — < 1%
13	eprints.umm.ac.id Internet	14 words — < 1%
14	www.teriin.org Internet	14 words — < 1%
15	issuu.com Internet	12 words — < 1%
16	Enkhtsetseg Munkhchuluun, Lasantha Meegahapola, Arash Vahidnia. "Impact on rotor	11 words — < 1%

Crossref

17	Hassan Alsharif, Mahdi Jalili, Kazi N. Hasan. "Power system frequency stability using optimal sizing and placement of Battery Energy Storage System under uncertainty", Journal of Energy Storage, 2022 Crossref	11 words — < 1%
18	Insu Kim, Ronald G. Harley. "The transient behavior of the Volt/Var control of photovoltaic systems for solar irradiation variations", 2016 IEEE Electrical Power and Energy Conference (EPEC), 2016 Crossref	11 words — < 1%
19	consultation.sepa.org.uk Internet	11 words — < 1%
20	etd.aau.edu.et Internet	11 words — < 1%
21	Ijaz, Muhammad. "Harmonic Detection and Mitigation in Power Systems using Wavelet Packet Transform.", King Fahd University of Petroleum and Minerals (Saudi Arabia), 2020 ProQuest	10 words — < 1%
22	Ujjwal Datta, Akhtar Kalam, Juan Shi. "Battery Energy Storage System Control for Mitigating PV Penetration Impact on Primary Frequency Control and State-of-Charge Recovery", IEEE Transactions on Sustainable Energy, 2020 Crossref	10 words — < 1%
23	mafiadoc.com Internet	10 words — < 1%

24	repositorio.unifei.edu.br Internet	10 words — < 1%
25	www.freepatentsonline.com Internet	10 words — < 1%
26	"Alternatives to the use of the crowbar circuit in DFIG based wind turbines during balanced voltage dips.", 'Universidade de Sao Paulo, Agencia USP de Gestao da Informacao Academica (AGUIA)' Internet	9 words — < 1%
27	Fanrong Wei, Zhiqiang Wan, Haibo He. "Cyber-Attack Recovery Strategy for Smart Grid Based on Deep Reinforcement Learning", IEEE Transactions on Smart Grid, 2019 Crossref	9 words — < 1%
28	G. Huang, S.-C. Hsieh. "A parallel HAD-textured algorithm for constrained economic dispatch control problems", IEEE Transactions on Power Systems, 1995 Crossref	9 words — < 1%
29	Mochamad, Rian Fatah. "Stability Assessment of Uncertain AC/DC System", The University of Manchester (United Kingdom) ProQuest	9 words — < 1%
30	Power Systems, 2014. Crossref	9 words — < 1%
31	Ryan, Nicole A.. "A Low Carbon Economy: Addressing Technical Challenges Spanning the Electricity and Steel Sectors", University of Michigan, 2021 ProQuest	9 words — < 1%
32	hdl.handle.net	